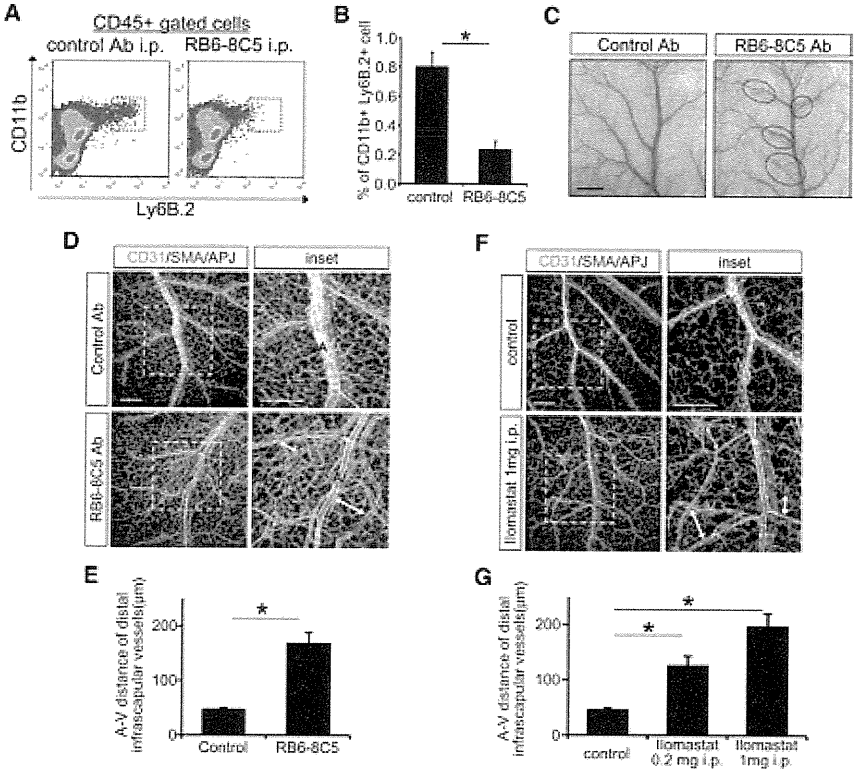

Figure 4. Neutrophil Lineage Cells Are Essential for A-V Alignment

(A) Representative flow cytometric plots of skin cells from E14.5 mouse embryos from pregnant mice treated with control Abs or RB6-8C5 Abs. The Ly6B.2$^+$ NLC fraction designated by CD45$^+$CD11b$^+$Ly6B.2$^+$ is gated in the red box.

(B) Quantitative evaluation of the CD45$^+$CD11b$^+$Ly6B.2$^+$ NLC population in the skin of embryos as observed in (A). Data represent the means ± SD; n = 3. *p < 0.01.

(C) Gross appearance of blood vessels in the back skin of adult mice (7–8 weeks of age) treated with control Abs or RB6-8C5 Abs. Note that veins are not completely aligned with arteries in RB6-8C5-treated mice (dotted ellipses). The scale bar represents 2 mm.

(D) CD31 (green), αSMA (red), and APJ (blue) staining of the back skin of an E15.5 mouse embryo treated with control Abs or RB6-8C5 Abs. Images on the right show a higher magnification of the areas indicated by the boxes. The scale bars represent 300 μm and 150 μm (insets).

(E) Quantitative evaluation of the distance between the artery and vein of distal infrascapular vessels in the back skin of E15.5 embryos treated with control Abs or RB6-8C5 Abs. Data represent the average ± SD; n = 15 from three mice per group. *p < 0.01.

(F) CD31 (green), αSMA (red), and APJ (blue) staining of back skin of an E15.5 mouse embryo treated with control solvent or Ilomastat (1 mg). Images on the right show a higher magnification of the areas indicated by the boxes. The scale bars represent 300 μm and 150 μm (insets).

(G) Quantitative evaluation of the distance between the artery and vein of distal infrascapular vessels in the back skin of E15.5 embryos treated with control solvent or the indicated concentrations of Ilomastat. Data represent the average ± SD; n = 12 from three mice per group. *p < 0.01.

permit venous displacement and formation of parallel juxtapositional A-V alignments.

Arterial-Venous Alignment Contributes to Thermoregulation during Both Cold and Heat Stress

An appropriate thermoregulatory system is essential for maintaining biological homeostasis in endotherms. Prolonged exposure to cold environmental conditions results in hypothermia, whereas heat stress triggers fatal symptoms, such as systemic contracture, elevation of core temperature, and severe rhabdomyolysis. "Precooling" of the arterial blood by juxtaposed veins was suggested long ago as a model for countercurrent heat exchange in physiological systems (Bazett et al., 1948a, 1948b) but has remained unproven. To explore the functional significance of A-V countercurrent heat exchange in thermoregulation, we evaluated the susceptibility to ambient temperature fluctuations of apelin/APJ signaling-deficient mice with disordered A-V alignment. To investigate the effects of cold stress, we exposed wild-type, *apelin*$^{-/-}$, and *APJ*$^{-/-}$ mice to a cold environment (4°C) and measured time-dependent changes of their rectal temperature. Rectal temperature was 38°C–39°C in these mice before exposure to cold ambient temperature. After a 6-hr exposure to cold, the temperature of the wild-type mice slightly decreased to 36.5°C ± 0.4°C but that of *apelin*$^{-/-}$ or *APJ*$^{-/-}$ mice rapidly dropped to 33.6°C ± 0.4°C or 33.3°C ± 0.6°C, respectively (Figure 6A). Next, to examine the effects of heat stress, mice were placed for up to 20 min in an environmental chamber in which the ambient temperature was maintained at 41°C. We determined heat sensitivity by monitoring the body surface temperature with an infrared camera. The results showed that heat stress caused a higher time-dependent increase in body temperature in *apelin*$^{-/-}$ or *APJ*$^{-/-}$ mice compared with wild-type mice (Figure 6B; Movies S1, S2, and S3). In particular, the increased body surface temperature of *apelin*$^{-/-}$ or *APJ*$^{-/-}$ mice 15 min after the heat stress protocol (7.1°C ± 1.2°C or 7.3°C ± 0.8°C, respectively) was higher than the corresponding values observed in wild-type mice (5.2°C ± 1.0°C) (Figure 6C). Under these conditions, all *apelin*$^{-/-}$ and *APJ*$^{-/-}$ mice suffered heat stroke-like episodes (16 or 18 min) characterized by impaired movement, difficulty in breathing,

(G) Quantitative evaluation of the Gr1$^+$CD45$^+$ neutrophil population in the back skin of E14.5 wild-type, *apelin*$^{-/-}$, or *APJ*$^{-/-}$ mouse embryos as observed in (B). Data represent the means ± SD; n = 3 embryos per group. n.s., not significant.

(H) qRT-PCR analysis of *MMP-9* mRNA expression in Ly6B.2$^+$ NLCs cultured in conditioned media from WT or *APJ*$^{-/-}$ ECs stimulated with apelin or PBS. Data represent the means ± SD; n = 3 independent samples per group. *p < 0.01.

See also Figure S3.

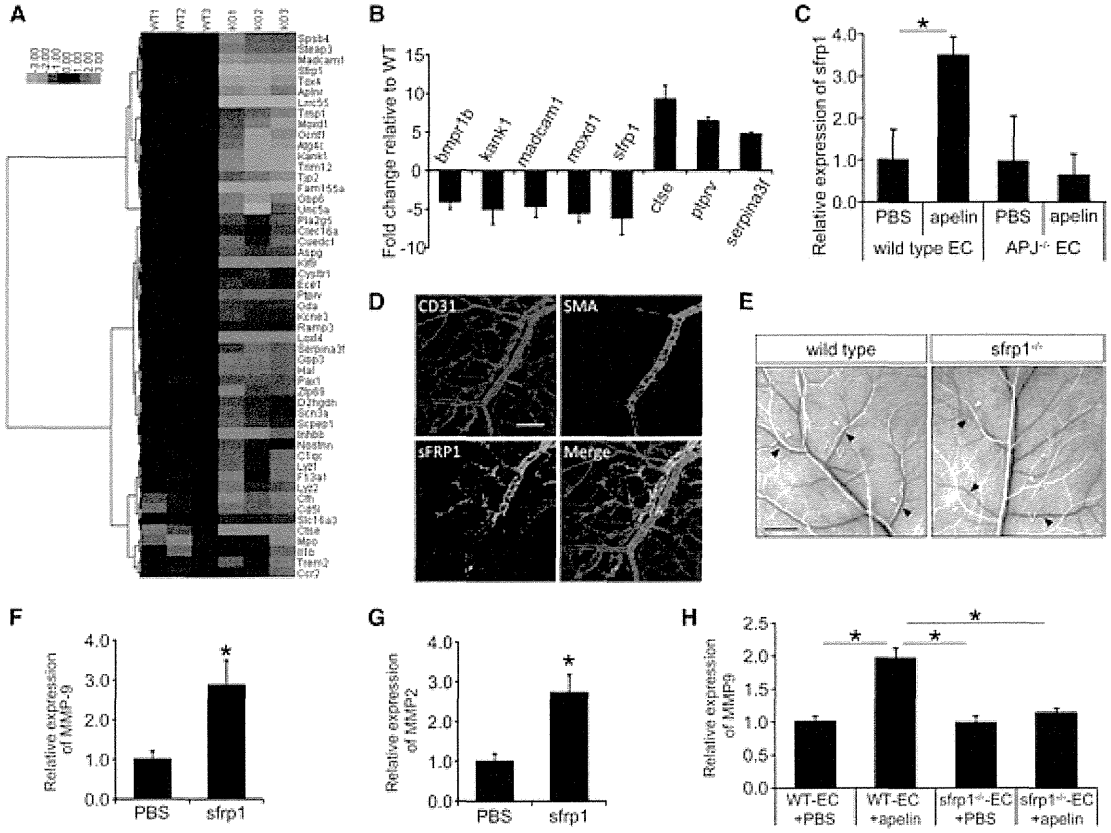

Figure 5. The Apelin-sFRP1 Axis Modulates MMP Expression

(A) Heat map of ECs from the back skin of E14.5 wild-type or *APJ*$^{-/-}$ mouse embryos as determined by DNA microarrays. Color intensity: red represents higher and green represents lower levels of mRNA relative to the reference ECs from wild-type mice (see color key in inset).

(B) qRT-PCR analysis of representative statistically significant ($p < 0.01$) genes. Target gene expression levels were normalized to *GAPDH*. Data represent the average ± SD; n = 3 independent embryos per group.

(C) Relative expression of *sfrp1* mRNA in cultured ECs from the back skin of E14.5 WT or *APJ*$^{-/-}$ embryos treated with vehicle or recombinant apelin for 24 hr. Data were normalized to *GAPDH*. Data represent the average ± SD; n = 3 independent samples per group. *$p < 0.01$.

(D) Immunohistochemical analysis of sFRP1 expression. CD31 (blue), αSMA (red), and sfrp1 (green) staining of the back skin of an E14.5 mouse embryo. The scale bar represents 100 μm.

(E) Gross appearance of blood vessels in the back skin of adult (7–8 weeks of age) wild-type and *sfrp1*$^{-/-}$ mice. Note that veins (black arrowheads) are not aligned with arteries (white arrowheads) in *sfrp1*$^{-/-}$ mice. The scale bar represents 2 mm.

(F and G) qRT-PCR analyses of *MMP-9* (F) or *MMP-2* (G) mRNA expression in cultured Ly6B.2^{+} NLCs from the back skin of E14.5 embryos stimulated with recombinant sFRP1. Data were normalized to *GAPDH*. Data represent the average ± SD; n = 3 independent cell lines per group. *$p < 0.01$.

(H) qRT-PCR analysis of *MMP-9* mRNA expression in Ly6B.2^{+} NLCs cultured in conditioned media from WT or *sfrp1*$^{-/-}$ ECs stimulated with apelin or PBS. Data represent the means ± SD; n = 3 independent samples per group. *$p < 0.01$.

See also Figure S4.

and systemic contractions, whereas wild-type animals under the same conditions had delayed episodes (Figure 6D).

It has been shown that apelin is also biosynthesized in neuronal cells and is suggested to play multiple roles in the central control of digestive behaviors, pituitary hormone release, and circadian rhythms (Reaux et al., 2002). To confirm that the phenotypes observed here in *apelin*$^{-/-}$ mice were caused by loss of apelin in blood vessels, we generated endothelial-specific knockout mice by crossing floxed *apelin* mice with the *Tie2-Cre* mouse line (Figures 6E–6G) (Schlaeger et al., 1997). Similar to conventional *apelin*$^{-/-}$ mice, blood vessels in the skin of the backs of adult *apelin*$^{flox/Y}$*:Tie2-Cre* mice had substantially abnormal A-V alignment compared to control mice (Figure 6H). We determined whether apelin deficiency specifically in vascular ECs affected different physiological functions associated with thermoregulation, such as cardiovascular function, adipose tissue development, neuronal function, and metabolic status. However, no significant physiological abnormalities were observed in *apelin*$^{flox/Y}$*:Tie2-Cre* mice, unlike those reported in *apelin*$^{-/-}$ or *APJ*$^{-/-}$ mice (data not shown) (Kuba et al., 2007; Roberts et al., 2009).

The cold stress test showed that body temperature was significantly decreased in *apelin*$^{flox/Y}$*:Tie2-Cre* mice (33.3°C ± 0.9°C) compared to *apelin*$^{flox/Y}$*:control* mice (36.1°C ± 0.2°C) (Figure 6I). Furthermore, when exposed to heat stress, these apelin mutant mice had significantly greater increases in body temperature than control mice, and more rapid development of heat stroke, as observed in the *apelin*$^{-/-}$ and *APJ*$^{-/-}$ mice (Figures

6J–6L; Movies S4 and S5). These results clearly demonstrate that countercurrent heat exchange between the artery and adjacent vein is indeed important for maintenance of body temperature and is crucial for resistance to heat stress.

DISCUSSION

Here we have shown that apelin released from arterial ECs stimulates APJ-positive venous ECs, resulting in the formation of parallel juxtapositional alignments between arteries and veins in the skin. Apelin has a direct effect on migration of APJ$^+$ venous ECs and induces sFRP1 production and MMP secretion from Ly6B.2$^+$ NLCs, resulting in ECM remodeling for venous displacement. Nonetheless, although *sfrp1*$^{-/-}$ mice showed disrupted A-V juxtapositioning, sFRP1 deficiency did not completely inhibit MMP expression in Ly6B.2$^+$ NLCs. This suggests that the apelin-sFRP1 axis is not the sole mechanism regulating the expression of this enzyme in the control of the juxtapositional alignment between arteries and veins.

We observed weak APJ expression in capillaries and strong expression in veins next to arteries. Interestingly, venous differentiation and morphogenesis occur normally in the absence of apelin/APJ signaling, despite defective A-V alignment. This suggests that apelin/APJ signaling and artery-vein interactions are not necessary for venous differentiation and angiogenesis. We previously reported that apelin regulates the enlargement of blood vessels and vascular permeability (Kidoya et al., 2008, 2010). In terms of caliber regulation, we reported that apelin deficiency affects small capillaries but does not influence arteriolae or venulae, as observed in this study. In contrast to the venous-specific expression of APJ, apelin production seemed to be restricted to arterial vessels covered with αSMA-positive mural cells. We previously reported that apelin expression is induced by angiopoietin-1 (Ang1); it is well known that Ang1 is predominantly produced by mural cells (Kidoya et al., 2008). Therefore, the stimulation of ECs by mural cells may initiate apelin production in arterial ECs. We showed that *APJ*$^{-/-}$ mice exhibit more profound abnormalities of A-V alignment than *apelin*$^{-/-}$ mice, and it was reported that some *APJ*$^{-/-}$ embryos die between E10.5 and E12.5 due to vascular defects (Kang et al., 2013) but that *apelin*$^{-/-}$ mice are born at the expected Mendelian ratio. This suggests the existence of apelin-independent mechanisms of APJ activation. Recent reports have concluded that APJ signaling is induced in response to mechanical stretching and to a second ligand, Toddler (ELABELA) (Scimia et al., 2012; Pauli et al., 2014; Chng et al., 2013). Mechanical forces, such as blood flow and extravascular tissue activity, are known to be important for the regulation of vascular formation. Blood flow might contribute to the patterning of the arteriovenous network through activation of APJ. The remodeling of blood vessels proceeds by multiple steps including fusion, intussusception, or regression of blood vessels and sprouting angiogenesis, among others. In these processes, matrix remodeling and movement of ECs are key steps for arrangement of vascular trees. We found that apelin plays a role in A-V alignment for vessels branching from larger arteriolae and venulae by inducing venous displacement. We speculate that venous displacement is induced by collective cell invasion into surrounding tissues utilizing venous EC migration toward the artery directly controlled by apelin/APJ and by matrix remodeling, that is, digestion of type IV collagen indirectly by apelin/APJ. Collective invasion of cells as a cohesive group is particularly prevalent during tissue remodeling such as morphological duct and gland formation in embryogenesis, skin wound repair, and cancer invasion (Friedl and Gilmour, 2009). Vascular displacement has been reported in granulation tissue during wound healing (Kilarski et al., 2009), but we propose that it also occurs in vascular remodeling during embryonic morphogenesis as described in this report. However, further molecular analysis to elucidate the mechanisms responsible for this vessel displacement is required.

Chaotic A-V alignment was observed not only in the skin vasculature but also in the hindlimb of *APJ*$^{-/-}$ mice. Thus, apelin/APJ signaling as detailed here for embryonic back skin likely contributes in the same manner to the coordinated patterning of arteries with veins in peripheral tissues. However, there are no significant abnormalities in the main arteries and veins branching from the aorta and vena cava and intercostal, cervical, and tail vessels in *apelin*$^{-/-}$ or *APJ*$^{-/-}$ mice. This suggests that the apelin/APJ system regulates only the vascular network formed by the remodeling process. Several previous studies have demonstrated that bidirectional repulsive ephrinB2-EphB4 signaling between arteries and veins is required for establishing the boundaries between them (Füller et al., 2003). Mice lacking ephrinB2 or EphB4 die in utero with similar phenotypes. These mice display grossly normal vasculogenesis of the major vessels as well as arrested remodeling of the primary vascular plexus, resulting in defective reciprocal communication between arteries and veins (Adams et al., 1999; Gerety et al., 1999; Wang et al., 1998). In contrast to such repulsive interactions, our study revealed that the apelin/APJ system mediates attractive interactions between arteries and veins. These data indicate that despite their close physical juxtaposition, separated arteries and veins have been constructed by different signals with opposing functions.

Several investigators over the years have suggested that the aligned vascular structure of arteries and veins in close proximity to each other contributes to thermoregulation by countercurrent heat exchange, mostly in the context of a cold environment (Bazett et al., 1948a, 1948b; Mitchell and Myers, 1968). However, theoretically, countercurrent heat exchange between arteries and veins may be important in both too-hot as well as too-cold conditions. Indeed, our apelin- or APJ-deficient mice, in which A-V alignment is disorganized, yielded results consistent with both these possibilities. Because APJ expression is also observed in poikilothermic zebrafish, we investigated the vascular patterning in the back skin of several animals other than mice, such as fish, birds, and reptiles, and found that A-V alignment only occurred in homeothermic animals (Figure S5A). This observation suggests that regulation of A-V alignment is crucial for thermoregulation and that the apelin/APJ system specifically functions for this purpose in homeotherm A-V alignment. We demonstrated the importance of A-V alignment in thermoregulation by using an endothelial-specific apelin-deficient mouse model. However, this does not exclude the possible existence of other factors that could account for differences in thermoregulation. Apelin itself also has numerous activities. In an attempt to exclude these possibilities, we confirmed that *apelin* EC knockout mice have no significant differences in metabolic

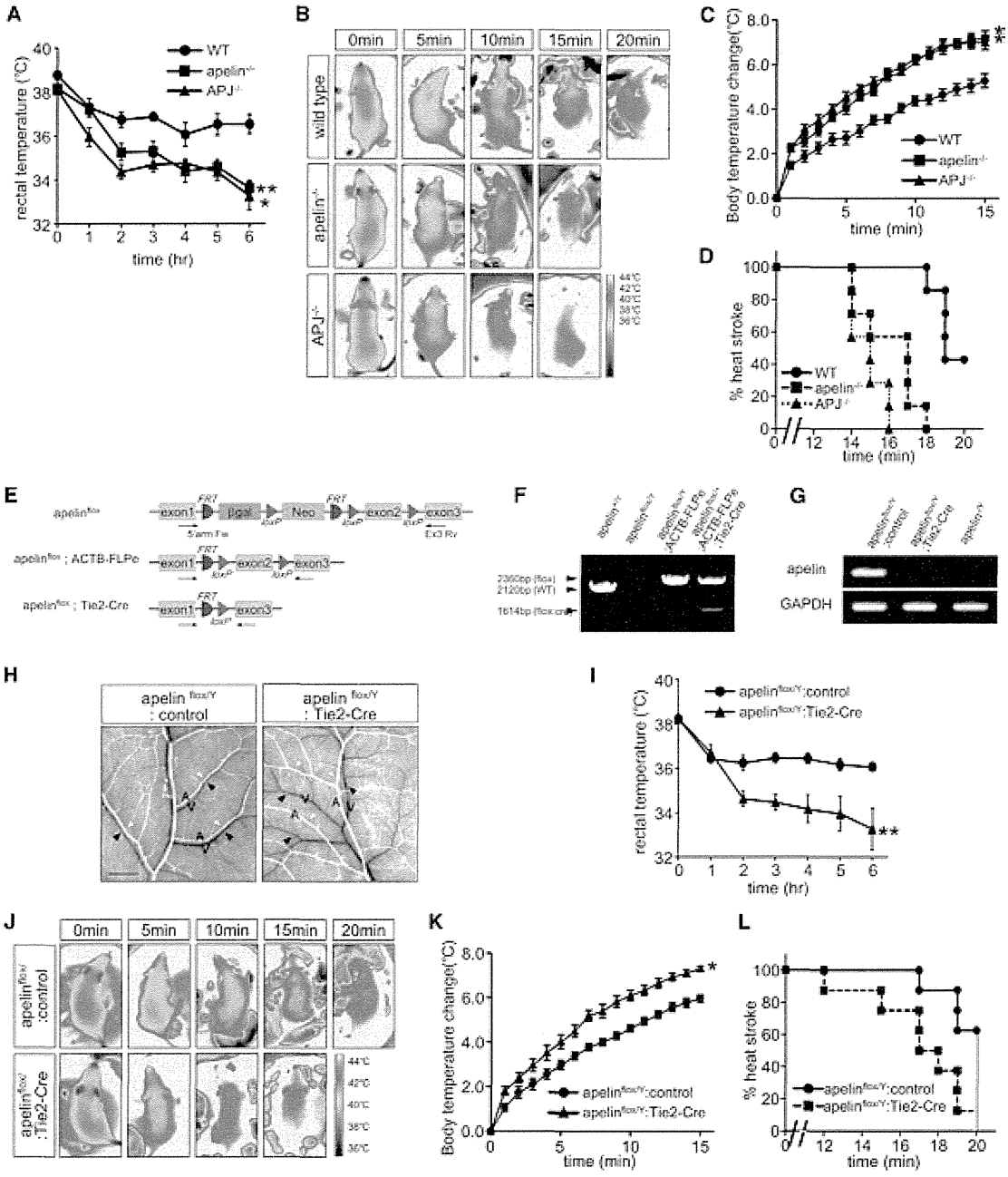

Figure 6. Contribution of Arterial-Venous Alignment to Thermoregulation

(A) Time-dependent changes of rectal temperature during acute cold stress. Wild-type, *apelin*$^{-/-}$, and *APJ*$^{-/-}$ mice were exposed to 4°C, after which their rectal temperature was monitored every hour. Data represent the average ± SE; n = 3 mice per group. *p < 0.01, **p < 0.05.

(B) Thermoregulatory response of wild-type, *apelin*$^{-/-}$, and *APJ*$^{-/-}$ mice subjected to heat stress (45°C). The temperature of the body surface was visualized and measured using infrared thermography.

(C) Increase in body temperature during heat stress in wild-type, *apelin*$^{-/-}$, and *APJ*$^{-/-}$ mice. Body surface temperature was monitored at 1-min intervals for 15 min. Data represent the average ± SE; n = 6 mice per group. *p < 0.01.

(D) Effects of increased body temperature caused by heat stress on severe heat stroke. The moment at which the mice remained immobile for more than 1 min was taken to be the onset of more severe heat stroke; data were analyzed using the Kaplan-Meier method. Note that *apelin*$^{-/-}$ and *APJ*$^{-/-}$ mice show a significant increase in the rate of more severe heat stroke ($p < 0.01$, log-rank test).

(E) Targeting strategy for the generation of *apelin*^{floxFRTNeo} and *apelin*^{flox} alleles.

(F) PCR analysis demonstrating the deletion of exon 2. The location and direction of the two primers used in the PCR analysis are also indicated by the arrows in (E).

(G) RT-PCR analysis of RNA extracted from ECs of E14.5 *apelin*$^{\Delta ex2}$ hemizygous embryos. Note that the intensity of the *apelin* mRNA in *apelin*$^{\Delta ex2}$ hemizygous ECs (*apelin*$^{flox/Y}$:*CAG-Cre*) is reduced, as compared with control (*apelin*$^{flox/Y}$:*control*) embryos, and that no truncated protein can be detected in *apelin*$^{-/-}$ ECs.

(legend continued on next page)

status, cardiac function, blood flow, and nervous system, unlike those previously reported in conventional *apelin*$^{-/-}$ or *APJ*$^{-/-}$ mice. Furthermore, brown fat development and tail vessel configuration, which are known to contribute to thermoregulation, were also normal. In addition, we verified the contribution of apelin/APJ-independent A-V misalignment to thermoregulation by using *sfrp1*$^{-/-}$ mice (Figures S5B–S5E).

We have previously reported that hematopoietic stem cells and hematopoietic progenitor cells promote angiogenesis and stabilize newly developed blood vessels, respectively, via the Ang1-Tie2 system (Takakura et al., 2000; Yamada and Takakura, 2006). Moreover, other hematopoietic lineages, such as monocyte macrophages, dendritic cells, mast cells, and others, can also affect angiogenesis by producing angiogenic cytokines and MMPs (Takakura and Kidoya, 2009). It has been suggested that platelets mediate the separation of blood vessels and lymphatic vessels (Abtahian et al., 2003; Bertozzi et al., 2010). Similar to the function of Ly6B.2^{+} NLCs for the induction of A-V alignment reported here, it is possible that other cells of the hematopoietic lineage are involved in alignment of arteries, veins, and lymphatics.

Thus far, molecular and cellular mechanisms of nerve-artery alignment have been suggested (Mukouyama et al., 2005) but parallel juxtapositional alignment between arteries and veins have not. Our data on the molecular analysis of A-V alignment and dependence on apelin and APJ expression open new avenues for research in this important area.

EXPERIMENTAL PROCEDURES

Cell Culture

The human promyelocytic leukemia cell line HL-60 was purchased from the RIKEN Cell Bank and maintained in RPMI-1640 medium (Sigma) supplemented with 10% heat-inactivated fetal bovine serum (Equitech-Bio). To induce differentiation of HL-60 cells, 1.3% DMSO was added for 72 hr. Mouse primary endothelial cells were seeded onto fibronectin-coated 35-mm dishes (Iwaki) in HuMedia-EG2.

Immunohistochemical Analysis

Tissue fixation and staining of sections or tissues with antibodies were performed as described previously (Takakura et al., 2000). An anti-CD31 monoclonal antibody (mAb) (BD Biosciences), anti-α-smooth muscle actin mAb (Dako), anti-apelin mAb (4G5), anti-APJ polyclonal Ab (Kidoya et al., 2008), anti-MMP-9 mAb (R&D Systems), anti-MMP-2 mAb (Merck Millipore), anti-ColIV mAb (Merck Millipore), anti-Ly6B.2 mAb (AbD Serotec), anti-F4/80 mAb (AbD Serotec), anti-neurofilament mAb (ARP), anti-sFRP1 mAb (Sigma-Aldrich), anti-EphB4 mAb (R&D Systems), and anti-Lyve1 Ab (MBL) were used for staining. Sections were examined by conventional microscopy (DM5500 B; Leica) or confocal microscopy (TCS/SP5; Leica), and images were acquired with a digital camera (DFC500; Leica). In all assays, isotype-matched Ig was used as a negative control, and it was confirmed that the positive signals were not derived from nonspecific background. Images were processed using Photoshop CS2 software (Adobe Systems) and analyzed using AngioTool (Zudaire et al., 2011) and ImageJ software (NIH). All images shown are representative of three to five independent experiments.

Flow Cytometric Analysis

Flow cytometry and isolation of endothelial cells and myeloid cells were performed as described previously (Kidoya et al., 2012; Naito et al., 2012). Fluorescence-labeled anti-CD45, -CD31, and -Gr1 mAbs (BD Biosciences) were used. Stained cells were sorted by FACSAria (BD Biosciences) and analyzed with FlowJo software (Tree Star). Dead cells were excluded by propidium iodide staining or analyses using the two-dimensional profile of the forward versus side scatter. Sorted cells were spun down onto glass slides using a Cytospin 4 instrument (Thermo Scientific) and stained with May-Grünwald-Giemsa (Muto Pure Chemicals).

Depletion of NLCs and Treatment with Matrix Metalloproteinase Inhibitor

The RB6-8C5 hybridoma, which produces a rat anti-mouse granulocyte mAb, was kindly provided by the Cell Resource Center for Biomedical Research of the Institute of Development, Aging and Cancer at Tohoku University. The antibody was purified from hybridoma culture supernatant. For in vivo depletion of NLCs, pregnant mice were treated intraperitoneally (i.p.) with 0.2 mg of mAb RB6-8C5 on days 10 and 13 of gestation as described previously (Daley et al., 2008). Control mice received rat IgG antibody (MBL). Blood vessels of back skin were analyzed at E14.5 or at 7–8 weeks (adult). Ilomastat (Merck Millipore), a broad-acting matrix metalloproteinase inhibitor, was i.p. administered to pregnant mice on days 12, 13, and 14 of gestation as a suspension in 4% carboxymethylcellulose (CMC) in saline. Control mice received 4% CMC in saline. Animals were housed in environmentally controlled rooms of the animal experimentation facility at Osaka University. All experiments were carried out under the guidelines of the Osaka University committee for animal and recombinant DNA experiments and were approved by the Osaka University Institutional Review Board.

Procedure for Mouse Arterial and Venous Microangiography

Mice were anesthetized with pentobarbital sodium (70 mg/kg i.p.) and fixed on an acrylic board in a supine position. After midline incision, the animal was perfused with heparinized saline through a 22-gauge needle inserted into the left ventricle for anticoagulation and exsanguination. Then, the hindlimb vasculature was perfused and fixed with 4% paraformaldehyde through the abdominal aorta and vein. Microangiograms were taken using a microfocus X-ray TV system (MFX-80HK; Hitex) as described previously (Shioyama et al., 2011). Barium sulfate was retrogradely injected into the femoral veins using an infusion pump until the vessels were filled with barium under fluoroscopic guidance, and the venogram was recorded in bitmap file format. After the contrast agent in the veins was completely flushed out by intraarterial saline infusion, barium was progradely injected into the femoral arteries and the arteriogram was acquired.

Murine Model of Heat Stroke and Hypothermia

The heat stress protocol consisted of exposing mice to a constant ambient temperature of 45°C in a prewarmed incubator for up to 20 min, a slight

(H) Gross appearance of blood vessels in the back skin of adult (7–8 weeks of age) *apelin*$^{flox/Y}$*:control* mice and *apelin*$^{flox/Y}$*:Tie2-Cre* mice. Arterial blood vessels were identified by injecting barium into the left ventricle. Veins (black arrowheads) are not aligned with arteries (white arrowheads) in endothelial-specific apelin-deficient mice (*apelin*$^{flox/Y}$*:Tie2-Cre* mice). The scale bar represents 2 mm.

(I) Time-dependent changes of rectal temperature during acute cold stress. The *apelin*$^{flox/Y}$*:control* mice and *apelin*$^{flox/Y}$*:Tie2-Cre* mice were exposed to 4°C and then their rectal temperature was monitored every hour. Data represent the average ± SE; n = 3 mice per group. $^{**}p < 0.05$.

(J) Thermoregulatory response of *apelin*$^{flox/Y}$*:control* mice and *apelin*$^{flox/Y}$*:Tie2-Cre* mice subjected to heat stress (45°C) visualized using infrared thermography.

(K) Increase in body temperature during heat stress in *apelin*$^{flox/Y}$*:control* mice and *apelin*$^{flox/Y}$*:Tie2-Cre* mice. Body surface temperature was monitored at 1-min intervals for 15 min. Data represent the average ± SE; n = 6 mice per group. $^{*}p < 0.01$.

(L) Effects of increased body temperature caused by heat stress on severe heat stroke. Severe heat stroke rates were analyzed using the Kaplan-Meier method ($p < 0.01$, log-rank test).

See also Figure S5 and Movies S1, S2, S3, S4, and S5.

modification of heat stroke protocols in mice (Mota et al., 2008). The body surface temperature was continuously monitored with an infrared camera (SC-620; FLIR Systems). Cold tolerance testing was performed by exposing mice to 5°C for 6 hr. Rectal temperature was measured by a thermistor thermometer inserted 2 cm into the rectum. This experiment was repeated at least nine times.

Statistical Analysis

All data are presented as the means ± SD. For statistical analysis, the Statcel 2 software package (OMS) was used, with ANOVA performed on all data, followed by the Tukey-Kramer multiple comparison test. When only two groups were compared, a two-sided Student's t test was used.

Additional experimental procedures and reagent information are presented in Supplemental Experimental Procedures.

SUPPLEMENTAL INFORMATION

Supplemental Information includes Supplemental Experimental Procedures, five figures, and five movies and can be found with this article online at http://dx.doi.org/10.1016/j.devcel.2015.02.024.

AUTHOR CONTRIBUTIONS

H.K. and N.T. designed and performed most of the experiments. H.N., F.M., D.Y., W.J., T.S., H.T., and M.S. supervised assays and performed some experiments. M.I. contributed *apelin*$^{flox/flox}$ mice; A.F. contributed *APJ*$^{-/-}$ mice; R.H.A. contributed *BMX-Cre* mice. H.K. and N.T. analyzed the results and wrote the manuscript.

ACKNOWLEDGMENTS

We thank Dr. S. Aizawa (RIKEN CDB Laboratory for Animal Resources and Genetic Engineering, Japan) and Dr. F. Stewart (Universitaet Dresden, Germany) for supplying mutant mice, and Dr. Y. Kanki and Dr. T. Minami (University of Tokyo, Japan) and Mr. R. Sasaki (Microeyes, Japan) for their help with data analysis. We are also grateful to Ms. K. Fukuhara, Ms. N. Fujimoto, and Ms. Y. Esaki for technical assistance. This work was supported by Grants-in-Aid for Scientific Research on Innovative Areas (23122511, 25122710, and 22112005) from the Ministry of Education, Culture, Sports, Science and Technology, a Grant-in-Aid for Young Scientists B (23701054) from the Japan Society for the Promotion of Science, and a Grant-in-Aid for the Research Center Network for Realization of Regenerative Medicine of the JST.

Received: September 28, 2014
Revised: January 22, 2015
Accepted: February 26, 2015
Published: April 23, 2015

REFERENCES

Abtahian, F., Guerriero, A., Sebzda, E., Lu, M.M., Zhou, R., Mocsai, A., Myers, E.E., Huang, B., Jackson, D.G., Ferrari, V.A., et al. (2003). Regulation of blood and lymphatic vascular separation by signaling proteins SLP-76 and Syk. Science *299*, 247–251.

Adams, R.H., Wilkinson, G.A., Weiss, C., Diella, F., Gale, N.W., Deutsch, U., Risau, W., and Klein, R. (1999). Roles of ephrinB ligands and EphB receptors in cardiovascular development: demarcation of arterial/venous domains, vascular morphogenesis, and sprouting angiogenesis. Genes Dev. *13*, 295–306.

Bates, D., Taylor, G.I., Minichiello, J., Farlie, P., Cichowitz, A., Watson, N., Klagsbrun, M., Mamluk, R., and Newgreen, D.F. (2003). Neurovascular congruence results from a shared patterning mechanism that utilizes Semaphorin3A and Neuropilin-1. Dev. Biol. *255*, 77–98.

Bazett, H.C., Love, L., Newton, M., Eisenberg, L., Day, R., and Forster, R., II. (1948a). Temperature changes in blood flowing in arteries and veins in man. J. Appl. Physiol. *1*, 3–19.

Bazett, H.C., Mendelson, E.S., Love, L., and Libet, B. (1948b). Precooling of blood in the arteries, effective heat capacity and evaporative cooling as factors modifying cooling of the extremities. J. Appl. Physiol. *1*, 169–182.

Bertozzi, C.C., Schmaier, A.A., Mericko, P., Hess, P.R., Zou, Z., Chen, M., Chen, C.Y., Xu, B., Lu, M.M., Zhou, D., et al. (2010). Platelets regulate lymphatic vascular development through CLEC-2-SLP-76 signaling. Blood *116*, 661–670.

Boucher, J., Masri, B., Daviaud, D., Gesta, S., Guigné, C., Mazzucotelli, A., Castan-Laurell, I., Tack, I., Knibiehler, B., Carpéné, C., et al. (2005). Apelin, a newly identified adipokine up-regulated by insulin and obesity. Endocrinology *146*, 1764–1771.

Carmeliet, P. (2003). Blood vessels and nerves: common signals, pathways and diseases. Nat. Rev. Genet. *4*, 710–720.

Chng, S.C., Ho, L., Tian, J., and Reversade, B. (2013). ELABELA: a hormone essential for heart development signals via the apelin receptor. Dev. Cell *27*, 672–680.

Chung, A.S., Lee, J., and Ferrara, N. (2010). Targeting the tumour vasculature: insights from physiological angiogenesis. Nat. Rev. Cancer *10*, 505–514.

Daley, J.M., Thomay, A.A., Connolly, M.D., Reichner, J.S., and Albina, J.E. (2008). Use of Ly6G-specific monoclonal antibody to deplete neutrophils in mice. J. Leukoc. Biol. *83*, 64–70.

Dufourcq, P., Couffinhal, T., Ezan, J., Barandon, L., Moreau, C., Daret, D., and Duplàa, C. (2002). FrzA, a secreted frizzled related protein, induced angiogenic response. Circulation *106*, 3097–3103.

Ehling, M., Adams, S., Benedito, R., and Adams, R.H. (2013). Notch controls retinal blood vessel maturation and quiescence. Development *140*, 3051–3061.

Friedl, P., and Gilmour, D. (2009). Collective cell migration in morphogenesis, regeneration and cancer. Nat. Rev. Mol. Cell Biol. *10*, 445–457.

Füller, T., Korff, T., Kilian, A., Dandekar, G., and Augustin, H.G. (2003). Forward EphB4 signaling in endothelial cells controls cellular repulsion and segregation from ephrinB2 positive cells. J. Cell Sci. *116*, 2461–2470.

Gerety, S.S., Wang, H.U., Chen, Z.F., and Anderson, D.J. (1999). Symmetrical mutant phenotypes of the receptor EphB4 and its specific transmembrane ligand ephrin-B2 in cardiovascular development. Mol. Cell *4*, 403–414.

Kälin, R.E., Kretz, M.P., Meyer, A.M., Kispert, A., Heppner, F.L., and Brändli, A.W. (2007). Paracrine and autocrine mechanisms of apelin signaling govern embryonic and tumor angiogenesis. Dev. Biol. *305*, 599–614.

Kang, Y., Kim, J., Anderson, J.P., Wu, J., Gleim, S.R., Kundu, R.K., McLean, D.L., Kim, J.D., Park, H., Jin, S.W., et al. (2013). Apelin-APJ signaling is a critical regulator of endothelial MEF2 activation in cardiovascular development. Circ. Res. *113*, 22–31.

Kasai, A., Shintani, N., Oda, M., Kakuda, M., Hashimoto, H., Matsuda, T., Hinuma, S., and Baba, A. (2004). Apelin is a novel angiogenic factor in retinal endothelial cells. Biochem. Biophys. Res. Commun. *325*, 395–400.

Kidoya, H., Ueno, M., Yamada, Y., Mochizuki, N., Nakata, M., Yano, T., Fujii, R., and Takakura, N. (2008). Spatial and temporal role of the apelin/APJ system in the caliber size regulation of blood vessels during angiogenesis. EMBO J. *27*, 522–534.

Kidoya, H., Naito, H., and Takakura, N. (2010). Apelin induces enlarged and nonleaky blood vessels for functional recovery from ischemia. Blood *115*, 3166–3174.

Kidoya, H., Kunii, N., Naito, H., Muramatsu, F., Okamoto, Y., Nakayama, T., and Takakura, N. (2012). The apelin/APJ system induces maturation of the tumor vasculature and improves the efficiency of immune therapy. Oncogene *31*, 3254–3264.

Kilarski, W.W., Samolov, B., Petersson, L., Kvanta, A., and Gerwins, P. (2009). Biomechanical regulation of blood vessel growth during tissue vascularization. Nat. Med. *15*, 657–664.

Klein, R. (2004). Eph/ephrin signaling in morphogenesis, neural development and plasticity. Curr. Opin. Cell Biol. *16*, 580–589.

Kuba, K., Zhang, L., Imai, Y., Arab, S., Chen, M., Maekawa, Y., Leschnik, M., Leibbrandt, A., Markovic, M., Schwaighofer, J., et al. (2007). Impaired heart

contractility in Apelin gene-deficient mice associated with aging and pressure overload. Circ. Res. *101*, e32–e42.

Lee, D.K., Cheng, R., Nguyen, T., Fan, T., Kariyawasam, A.P., Liu, Y., Osmond, D.H., George, S.R., and O'Dowd, B.F. (2000). Characterization of apelin, the ligand for the APJ receptor. J. Neurochem. *74*, 34–41.

Li, W., Kohara, H., Uchida, Y., James, J.M., Soneji, K., Cronshaw, D.G., Zou, Y.R., Nagasawa, T., and Mukouyama, Y.S. (2013). Peripheral nerve-derived CXCL12 and VEGF-A regulate the patterning of arterial vessel branching in developing limb skin. Dev. Cell *24*, 359–371.

Lin, F.J., Tsai, M.J., and Tsai, S.Y. (2007). Artery and vein formation: a tug of war between different forces. EMBO Rep. *8*, 920–924.

Mitchell, J.W., and Myers, G.E. (1968). An analytical model of the counter-current heat exchange phenomena. Biophys. J. *8*, 897–911.

Mota, R.A., Hernández-Espinosa, D., Galbis-Martinez, L., Ordoñez, A., Miñano, A., Parrilla, P., Vicente, V., Corral, J., and Yélamos, J. (2008). Poly(ADP-ribose) polymerase-1 inhibition increases expression of heat shock proteins and attenuates heat stroke-induced liver injury. Crit. Care Med. *36*, 526–534.

Mukouyama, Y.S., Shin, D., Britsch, S., Taniguchi, M., and Anderson, D.J. (2002). Sensory nerves determine the pattern of arterial differentiation and blood vessel branching in the skin. Cell *109*, 693–705.

Mukouyama, Y.S., Gerber, H.P., Ferrara, N., Gu, C., and Anderson, D.J. (2005). Peripheral nerve-derived VEGF promotes arterial differentiation via neuropilin 1-mediated positive feedback. Development *132*, 941–952.

Naito, H., Kidoya, H., Sakimoto, S., Wakabayashi, T., and Takakura, N. (2012). Identification and characterization of a resident vascular stem/progenitor cell population in preexisting blood vessels. EMBO J. *31*, 842–855.

Nathan, E., and Tzahor, E. (2009). sFRPs: a declaration of (Wnt) independence. Nat. Cell Biol. *11*, 13.

Nozawa, H., Chiu, C., and Hanahan, D. (2006). Infiltrating neutrophils mediate the initial angiogenic switch in a mouse model of multistage carcinogenesis. Proc. Natl. Acad. Sci. USA *103*, 12493–12498.

Pasquale, E.B. (2005). Eph receptor signalling casts a wide net on cell behaviour. Nat. Rev. Mol. Cell Biol. *6*, 462–475.

Pauli, A., Norris, M.L., Valen, E., Chew, G.L., Gagnon, J.A., Zimmerman, S., Mitchell, A., Ma, J., Dubrulle, J., Reyon, D., et al. (2014). Toddler: an embryonic signal that promotes cell movement via Apelin receptors. Science *343*, 1248636.

Poliakov, A., Cotrina, M., and Wilkinson, D.G. (2004). Diverse roles of Eph receptors and ephrins in the regulation of cell migration and tissue assembly. Dev. Cell *7*, 465–480.

Reaux, A., Gallatz, K., Palkovits, M., and Llorens-Cortes, C. (2002). Distribution of apelin-synthesizing neurons in the adult rat brain. Neuroscience *113*, 653–662.

Roberts, E.M., Newson, M.J., Pope, G.R., Landgraf, R., Lolait, S.J., and O'Carroll, A.M. (2009). Abnormal fluid homeostasis in apelin receptor knockout mice. J. Endocrinol. *202*, 453–462.

Rosas, M., Thomas, B., Stacey, M., Gordon, S., and Taylor, P.R. (2010). The myeloid 7/4-antigen defines recently generated inflammatory macrophages and is synonymous with Ly-6B. J. Leukoc. Biol. *88*, 169–180.

Saint-Geniez, M., Argence, C.B., Knibiehler, B., and Audigier, Y. (2003). The msr/apj gene encoding the apelin receptor is an early and specific marker of the venous phenotype in the retinal vasculature. Gene Expr. Patterns *3*, 467–472.

Schlaeger, T.M., Bartunkova, S., Lawitts, J.A., Teichmann, G., Risau, W., Deutsch, U., and Sato, T.N. (1997). Uniform vascular-endothelial-cell-specific gene expression in both embryonic and adult transgenic mice. Proc. Natl. Acad. Sci. USA *94*, 3058–3063.

Schulz, C., Gomez Perdiguero, E., Chorro, L., Szabo-Rogers, H., Cagnard, N., Kierdorf, K., Prinz, M., Wu, B., Jacobsen, S.E., Pollard, J.W., et al. (2012). A lineage of myeloid cells independent of Myb and hematopoietic stem cells. Science *336*, 86–90.

Scimia, M.C., Hurtado, C., Ray, S., Metzler, S., Wei, K., Wang, J., Woods, C.E., Purcell, N.H., Catalucci, D., Akasaka, T., et al. (2012). APJ acts as a dual receptor in cardiac hypertrophy. Nature *488*, 394–398.

Shioyama, W., Nakaoka, Y., Higuchi, K., Minami, T., Taniyama, Y., Nishida, K., Kidoya, H., Sonobe, T., Naito, H., Arita, Y., et al. (2011). Docking protein Gab1 is an essential component of postnatal angiogenesis after ischemia via HGF/c-Met signaling. Circ. Res. *108*, 664–675.

Takakura, N., and Kidoya, H. (2009). Maturation of blood vessels by haematopoietic stem cells and progenitor cells: involvement of apelin/APJ and angiopoietin/Tie2 interactions in vessel caliber size regulation. Thromb. Haemost. *101*, 999–1005.

Takakura, N., Watanabe, T., Suenobu, S., Yamada, Y., Noda, T., Ito, Y., Satake, M., and Suda, T. (2000). A role for hematopoietic stem cells in promoting angiogenesis. Cell *102*, 199–209.

Tazzyman, S., Lewis, C.E., and Murdoch, C. (2009). Neutrophils: key mediators of tumour angiogenesis. Int. J. Exp. Pathol. *90*, 222–231.

Tucker, B., Hepperle, C., Kortschak, D., Rainbird, B., Wells, S., Oates, A.C., and Lardelli, M. (2007). Zebrafish Angiotensin II Receptor-like 1a (agtrl1a) is expressed in migrating hypoblast, vasculature, and in multiple embryonic epithelia. Gene Expr. Patterns *7*, 258–265.

van Hinsbergh, V.W., Engelse, M.A., and Quax, P.H. (2006). Pericellular proteases in angiogenesis and vasculogenesis. Arterioscler. Thromb. Vasc. Biol. *26*, 716–728.

Wang, H.U., Chen, Z.F., and Anderson, D.J. (1998). Molecular distinction and angiogenic interaction between embryonic arteries and veins revealed by ephrin-B2 and its receptor Eph-B4. Cell *93*, 741–753.

Yamada, Y., and Takakura, N. (2006). Physiological pathway of differentiation of hematopoietic stem cell population into mural cells. J. Exp. Med. *203*, 1055–1065.

Zudaire, E., Gambardella, L., Kurcz, C., and Vermeren, S. (2011). A computational tool for quantitative analysis of vascular networks. PLoS ONE *6*, e27385.

The Preventive Effect of Endovascular Treatment for Recurrent Hemorrhage in Patients with Spinal Cord Arteriovenous Malformations

Y. Niimi, H. Matsukawa, N. Uchiyama, and A. Berenstein

ABSTRACT

BACKGROUND AND PURPOSE: Spinal cord AVMs represent rare and insufficiently studied pathologic entities. Embolization is thought to play an important role in the management of spinal cord AVMs. Factors for recurrent hemorrhage and the impact of endovascular treatment on prevention of recurrent hemorrhage remain to be confirmed. We aimed to assess recurrent hemorrhagic incidence of spinal cord AVMs and its prevention by endovascular treatment.

MATERIALS AND METHODS: We reviewed 80 patients with spinal cord AVMs by spinal cord angiography who had hemorrhage before the first endovascular treatment at New York University Medical Center, Beth Israel Medical Center, or Roosevelt Hospital in New York. We compared the baseline and radiologic characteristics of patients with and without recurrent hemorrhage by the log-rank test and the Cox proportional hazards model.

RESULTS: We observed recurrent hemorrhage in 35 (44%) patients (1/41 patients with endovascular treatment and 34/39 patients without endovascular treatment). The median length of total follow-up was 659 days (interquartile range, 129–2640 days), and the median length from first-to-recurrent hemorrhage was 369 days (interquartile range, 30–1596 days). The log-rank test revealed that endovascular treatment and venous thrombosis reduced recurrent hemorrhage, and associated aneurysm was related to recurrent hemorrhage. Even in multivariate analysis, the endovascular treatment reduced (hazard ratio, 0.027; $P < .0001$) and associated aneurysm increased (hazard ratio, 3.4; $P = .044$) the risk of recurrent hemorrhage.

CONCLUSIONS: Endovascular embolization is the first choice of treatment for spinal cord AVMs and is effective in preventing recurrent hemorrhage.

ABBREVIATIONS: ASA = anterior spinal artery; NBCA = *n*-butyl 2-cyanoacrylate; SCAVM = spinal cord AVM

Spinal cord AVMs (SCAVMs) represent rare and insufficiently studied pathologic entities characterized by considerable variation.[1] Insufficient study of this disease is associated with the rarity and complexity of its diagnosis.[2,3] Spinal cord arteriovenous fistula is a direct communication between arteries and veins, while spinal cord arteriovenous malformation in its narrow denotation has a nidus, an abnormal vascular network interposed between arteries and veins. On some occasions, both AVF and AVM constitute a shunt, which is also called AVM in its broader meaning.[4] Spinal cord AVFs and AVMs manifest with sudden or gradual deterioration of sensorimotor function in the extremities and/or of micturition, defecation, or sexual function due mainly to venous hypertension/ischemia and, in some cases, arterial steel, hemorrhage, or mass effect.[4]

There has been advancement in endovascular treatment of SCAVM, including monitoring systems. Treatment of an SCAVM aims to decrease the risk of hemorrhage and arrest the progression of neurologic deterioration.[5] Embolization is thought to play an important role in the management of SCAVMs, both as a primary treatment and as an adjunct to surgical excision. However, complete cure of SCAVMs by endovascular embolization is exceptional except for spinal cord AVFs, and endovascular treatment often results in partial obliteration of the lesion by target embolization. Target embolization aims at occluding dangerous structures causing hemorrhage or neurologic symptoms, such as aneurysms, high-flow fistulas, and nerve root lesions for radicular pain. To date, various studies investigated the factors related to

Received July 31, 2014; accepted after revision February 4, 2015.

From the Departments of Neuroendovascular Therapy (Y.N.) and Neurosurgery (H.M.), St. Luke's International Hospital, Tokyo, Japan; Department of Neurosurgery (N.U.), Kanazawa University, Kanazawa, Japan; and Center for Endovascular Surgery (A.B.), Roosevelt Hospital, New York, New York.

Please address correspondence to Yasunari Niimi, MD, Department of Neuroendovascular Therapy, St. Luke's International Hospital, 9-1 Akashi-cho, Chuo-ku, Tokyo 104-8560, Japan; e-mail address: yasunm@luke.ac.jp

http://dx.doi.org/10.3174/ajnr.A4396

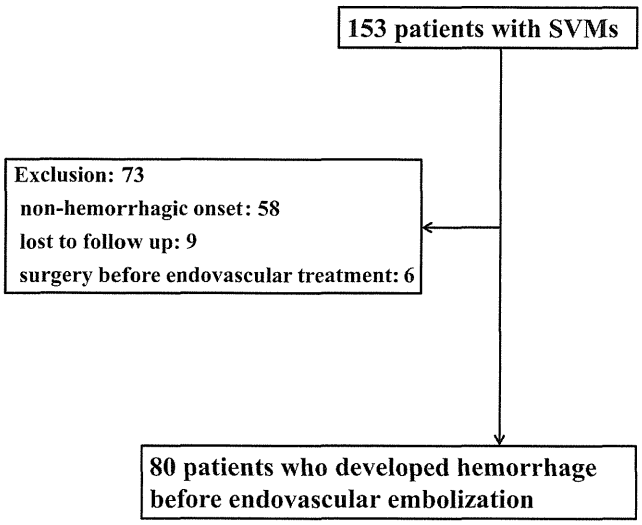

FIG 1. Exclusion criteria of the present study. SVM indicates spinal vascular malformation.

initial hemorrhage.[6-10] However, factors for recurrent hemorrhage and the impact of endovascular treatment on prevention of recurrent hemorrhage remain to be confirmed. The purpose of this study was to assess the recurrent hemorrhagic incidence of SCAVMs and its prevention by endovascular treatment.

MATERIALS AND METHODS

The study is reported on the basis of criteria from the Strengthening the Reporting of Observational Study in Epidemiology statement.[11]

Study Participants

We retrospectively reviewed 153 patients diagnosed with SCAVM by spinal cord angiography at centers where the senior author worked (New York University Medical Center, Beth Israel Medical Center, or Roosevelt Hospital in New York) between April 1980 and October 2010. Exclusion criteria are shown in Fig 1. After exclusions, we analyzed 80 patients with SCAVMs who had hemorrhage before the first endovascular treatment.

Clinical Characteristics

We collected the following data: age, sex, the presence of SCAVM-related syndrome, endovascular treatment after the first hemorrhage or radiation therapy, and radiologic characteristics. We defined pediatrics as younger than 18 years of age.

Radiologic characteristics included hemorrhage type, detailed diagnosis, lesion level, the presence of an associated aneurysm, venous thrombosis, venous stricture, venous ectasia, and venous hypertension.

Improvement of Angiographic and Embolization Techniques

There has been improvement in angiographic and embolization techniques during the 30 years of the study and continuous improvement in knowledge of disease, angiographic imaging quality, endovascular equipment including microcatheters, microguidewires, embolic agents, and monitoring systems. We started by using guidewire-assisted and flow-guided microcatheters in the late 1980s. As a monitoring system, somatosensory evoked potentials introduced in the mid-1980s, and transcranial motor evoked potentials, in the mid-1990s as well as the provocative testing method.[12] We switched from isobutyl cyanoacrylate to *n*-butyl 2-cyanoacrylate (NBCA) as a liquid embolic agent in the late 1980s. Detachable coils became available for certain diseases in the early 1990s. All these improvements enhanced the safety and adequacy of endovascular occlusion of SCAVMs. However, our conceptual approach for endovascular treatment of an SCAVM (ie, partial targeted embolization) is, in principle, unchanged during the 30 years of the study because we still have difficulty in completely obliterating an SCAVM by embolization itself. Therefore, we decided to analyze all cases of SCAVMs during 30 years.

Current Angiographic/Embolization Protocol

All angiographic procedures were performed with the patients under general anesthesia with neuroleptic agents and neurophysiologic monitoring, including somatosensory evoked potentials and transcranial motor evoked potentials. Superselective catheterization of the appropriate feeding pedicles was performed by using a microcatheter before embolization to analyze the vascular anatomy of the lesion. Pharmacologic provocative testing was performed with superselective injection of amobarbital sodium and lidocaine when indicated. The details of the indication, technique, and results of neurophysiologic monitoring and provocative testing for SCAVMs have been described previously.[12] After hemorrhage with neurologic deficits, patients were treated conservatively until their neurologic deficits became stabilized, and we then performed endovascular treatment if indicated. We perform targeted partial embolization for nidus-type SCAVMs to close aneurysms and fistulas to prevent hemorrhage and improve spinal cord hemodynamics to treat symptomatic myelopathy/venous hypertension. Complete angiographic cure is not the goal with most intradural lesions with the exception of AVFs. *n*-butyl 2-cyanoacrylate was the main embolic agent for both intra- and extradural lesions. Particulate embolization was used when NBCA embolization was not feasible on the basis of the flow dynamics of the lesion. Coils were used for embolization of aneurysms, high-flow fistulas, and protection of the normal vascular territories when embolizations were performed from proximal positions (nonintranidal). Ethylene-vinyl alcohol copolymer (Onyx; Covidien, Irvine, California) was not used for intradural lesions. The embolization procedure was repeated in a staged fashion if considered preferable.

Outcome

The treatment results were confirmed by angiography after embolization. MR imaging was also performed if indicated. Clinical follow-up was performed in a multidisciplinary clinic attended by both interventional neuroradiologists and neurosurgeons. In case of any clinical suspicion of recurrence or progression of the disease, MR imaging or angiography or both were repeated at that time. Repeat embolization was performed on the basis of the angiographic findings. Annual follow-up MR imaging was performed if the patient was neurologically stable. If there was any change in the appearance, spinal angiography was performed with the intent to treat.

Table 1: Duration between initial and recurrent hemorrhage in patients with SCAVMs

Duration	No. (n = 35)	Percentage
<7 Days	6	18
8–31 Days	5	14
1–6 Months	2	5.7
6 Months to 1 year	4	11
1–2 Years	2	5.7
2–3 Years	3	8.6
>3 Years	13	37

The end points were survival without recurrent hemorrhage from SCAVMs.

Statistical Analysis

Statistical analysis was performed by using SPSS for Mac (Version 21.0; IBM, Armonk, New York). Variables are expressed as mean ± SD, median (interquartile range: 25th–75th percentile), or number of patients (percentage) as appropriate. The normality of the data was evaluated by using the Shapiro-Wilk test. We performed receiver operating characteristics curve analysis for age and the binary end point of recurrent hemorrhage, and we selected the age cutoff point that optimized sensitivity and specificity.

We compared the baseline and radiologic characteristics of patients with and without recurrent hemorrhage by the log-rank test and performed multivariate analysis by the Cox proportional hazards model by using variables that were marginally or significantly associated with progression on the log-rank test ($P < .20$). The probability of freedom from recurrent hemorrhage was estimated by using the Kaplan-Meier method; comparisons of the survival curves by the number of factors were performed by using the log-rank test. Differences were considered significant at $P < .05$ for a 95% CI.

RESULTS

Forty-four patients (55%) presented with subarachnoid hemorrhage and 36 (45%) presented with hematomyelia. Types of initial hemorrhage were not related to recurrent hemorrhage ($P = .54$). We observed recurrent hemorrhage in 35 (44%) patients, including 1 of 41 patients treated by embolization and 34 of 39 patients not treated by embolization. The median length of total follow-up was 659 days (interquartile range, 129–2640 days), and the median length from the first-to-recurrent hemorrhage was 369 days (interquartile range, 30–1596 days). We found that 31% of patients rebled within 1 month of the first hemorrhage and 40% of them rebled in >3 years (Table 1). Associated diseases were noted in several patients: spinal arterioveonous metameric syndrome in 10 patients (13%) with recurrent hemorrhage and in 9 (20%) without recurrent hemorrhage; Klippel-Trenaunay-Weber syndrome in 1 (2.9%) with recurrent hemorrhage, not seen in those without recurrent hemorrhage; and Osler-Weber-Rendu disease in 1 (2.9%) with recurrent hemorrhage, not seen in those without recurrent hemorrhage. No significant difference was found among these associated diseases and recurrent hemorrhage ($P = .94$). Radiation therapy was performed in 3 patients (8.6%) with recurrent hemorrhage and was not performed in patients without recurrent hemorrhage ($P = .42$). Clinical and radiologic characteristics of 80 patients with and without recurrent hemorrhage are shown in Table 2. The log-rank test revealed that endovascular treatment (Fig 2) and venous thrombosis significantly and marginally reduced recurrent hemorrhage, respectively, and an associated aneurysm was significantly related to recurrent hemorrhage. Even in multivariate analysis, the endovascular treatment reduced and associated aneurysm increased the risk of recurrent hemorrhage (Table 3).

Illustrative Case

This male patient initially presented with a spinal subarachnoid hemorrhage at 11 years of age. A diagnosis of an SCAVM was made by MR imaging and spinal angiography at that time, but no treatment was performed. He then experienced 3 spinal subarachnoid hemorrhages in a month, documented by spinal tap at 14 years of age. He was then referred to us for endovascular treatment. On admission, he was neurologically intact. Angiographic study demonstrated a nidus-type SCAVM at the T2 spinal level supplied mainly by the anterior spinal artery (ASA) with multiple intranidal aneurysms (Fig 3*A*). Superselective angiography from a feeder coming off the ASA failed to demonstrate the aneurysms (Fig 3*B*, *-C*). Superselective angiography from the ASA near the feeder origin demonstrated an intranidal aneurysm supplied by a branch of the ASA different from the feeder that was previously catheterized (Fig 3*D*). Because of the inability to superselectively catheterize the feeder supplying the aneurysm, embolization from the ASA near the origin of the feeder was performed by using NBCA (Fig 3*E*). Control angiography after the embolization showed decreased size of the AVM without opacification of the aneurysms. The ASA was disconnected for a short segment, but the distal segment was opacified through the collateral. The remaining nidus was also opacified by the ASA and the posterior spinal artery opacified from the left T10 and the left T8 intercostal artery, respectively (not shown). The patient remained neurologically intact and had no further hemorrhage during the follow-up for 6 years after the embolization.

DISCUSSION

The results of the present study showed that the endovascular treatment reduced and associated aneurysm increased the risk of recurrent hemorrhage in patients with hemorrhagic SCAVM.

Hemorrhage

The congenital nature of SCAVMs in their form at presentation is also debatable,[13] because their appearance after hemorrhage may reflect the result of decompensation of the vasculature lesion and the surrounding spinal cord, which occurred after birth. It has previously been reported that once a patient hemorrhages, the incidence of recurrent hemorrhage is very high.[14] The overall annual hemorrhage rate was 4%, increasing to 10% for spinal glomus (type 2) SCAVMs with previous hemorrhage,[8] and lesions with initial hemorrhage also had a greater annual rate of recurrent hemorrhage (5.6%) compared with nonhemorrhagic lesions (0.4%) in spinal cord AVF.[15] Our series showed an higher incidence of hemorrhage: 58% as the initial symptom and 66% before treatment. In the literature, initial hemorrhage was encountered in 70% of pediatric and 27%–45% of adult patients with

Table 2: Univariate freedom from recurrent hemorrhage of SCAVMs[a]

Variables	Total (*n* = 80)	Recurrent Hemorrhage (+) (*n* = 35)	Recurrent Hemorrhage (-) (*n* = 45)	Unadjusted *P* Value
Baseline characteristics				
Median age (yr) (IQR)	20 (10–32)	18 (8–25)	21 (15–38)	
Pediatric	30 (38)	16 (46)	14 (31)	.87
Male	31 (39)	12 (34)	19 (42)	.73
Endovascular embolization[b]	41 (51)	1 (2.9)	40 (89)	<.0001
Radiologic characteristics				
Subclassification				.51
SCAVM	63 (79)	31 (89)	32 (71)	
SCAVF, single hole	7 (8.8)	1 (2.9)	6 (13)	
SCAVF, multiple holes	10 (13)	4 (11)	6 (13)	
SCAVM level				.92
Cranial-cervical	2 (2.5)	1 (2.9)	1 (2.2)	
Cervical	33 (41)	16 (46)	17 (39)	
Cervical-thoracic	1 (1.3)	0	1 (2.2)	
Thoracic	31 (39)	13 (37)	18 (40)	
Thoracic-lumbar	9 (11)	4 (11)	5 (11)	
Lumbar	4 (5.0)	1 (2.9)	3 (6.7)	
Associated aneurysm[b]	56 (70)	31 (89)	25 (56)	.049
Venous thrombosis[b]	7 (8.8)	1 (2.9)	6 (13)	.19
Venous stricture	2 (2.5)	0	2 (4.4)	.21
Venous ectasia	16 (20)	7 (20)	9 (20)	.24
Venous hypertension	16 (20)	7 (20)	9 (20)	.66

Note:—SCAVF indicates spinal cord AVF; IQR, interquartile range 25th–75th percentile.
[a] Data are expressed as number of lesions (%), unless otherwise indicated.
[b] Variables related to the recurrent hemorrhage by log-rank test ($P < .20$).

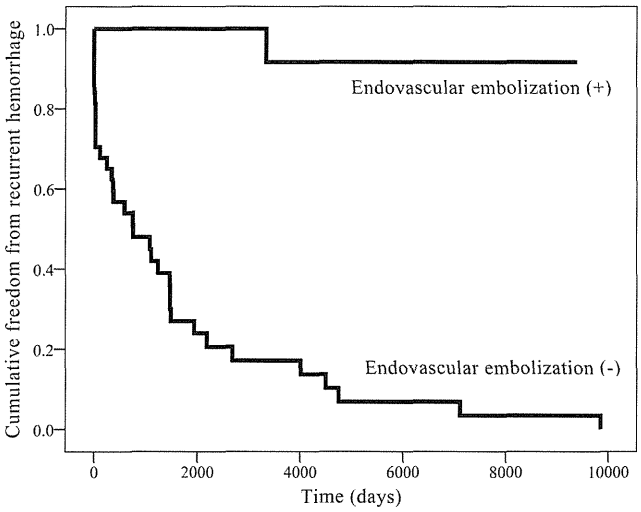

FIG 2. Kaplan-Meier plot of cumulative freedom from the progression by endovascular embolization.

Table 3: Multivariate analyses using the Cox proportional hazards model for recurrent hemorrhage from SCAVMs

Variable	Adjusted HR	95% CI	Multivariable Adjusted *P* Value
Endovascular treatment[a]	0.027	0.0040–0.19	<.0001
Associated aneurysm[a]	3.4	1.2–11	.044
Venous thrombosis	0.61	0.082–4.5	.63

Note:—HR indicates hazard ratio.
[a] Variables related to recurrent hemorrhage.

SCAVMs, 20%–37% of pediatric and adult patients with AVF, and 50% of pediatric and adult patients with glomus-type AVMs.[6,8,9,15,16] In the present study, initial hemorrhage was seen in 52% of all patients, 51% of pediatric patients, and 53% of adults, and this finding supported the results of the previous studies. Previous study also showed that early (within the 12 months after the first hemorrhage) recurrent hemorrhage was seen in 4.8% of pediatric patients and in 3.6% of adults, and late (>1 year after the first hemorrhage) recurrent hemorrhage was seen in 4.8% of pediatric patients and 14% of adults with SCAVM.[6] However, early recurrent hemorrhage was seen in 20% of pediatric patients and in 20% of adults, and late recurrent hemorrhage was seen in 33% of pediatric patients and in 18% of adults in the present study. This result indicated that the rate of recurrent hemorrhage from SCAVMs in both pediatric patients and adults was higher than previously expected.

Recurrent hemorrhages after endovascular embolization were seen in 4%, and all of these were cervical SCAVMs in the previous study.[17] We observed that only 1 of 41 patients (2.4%) had recurrent hemorrhage among those who underwent endovascular treatment, as opposed to 34 of 39 patients (87.2%) without endovascular treatment. Many of those who had rehemorrhage without endovascular treatment were treated by endovascular embolization without further hemorrhage in our series (data not shown). The low incidence of hemorrhage after partial embolization of SCAVMs has also been reported by other authors.[5]

Associated aneurysms of the feeding arteries and nidus are common in SCAVMs.[7] Spinal cord artery and intranidal aneurysms are associated with a high risk for hemorrhage in SCAVMs.[7] Some studies have shown that SCAVM-related arterial aneurysms (distinct from false aneurysms) were associated with initial hemorrhage,[6,8,14,18] though one group of authors showed that arterial aneurysms (distinct from false aneurysms) were not related to hemorrhagic presentation.[16] It was also reported that recurrent hemorrhages were mostly due to rerupture of an associated false aneurysm in SCAVMs.[6] The results of the present study showed that associated aneurysms were seen in 89% of patients with recurrent hemorrhage and in 56% of those without recurrent hemorrhage and supported the relationship between associated aneurysms and recurrent hemorrhage in patients with an SCAVM.

Although venous architectural factors (either venous ectasias or venous stricture) were most often associated with initial hemorrhage,[16] they were not related to recurrent hemorrhage in the present study.

Endovascular Treatment

Embolization of an SCAVM is performed once the endovascular "dissection" of the SCAVM with microcatheter angiography and provocative testing is complete. Analysis of vascular anatomy is most important for safe embolization, but electrophysiologic

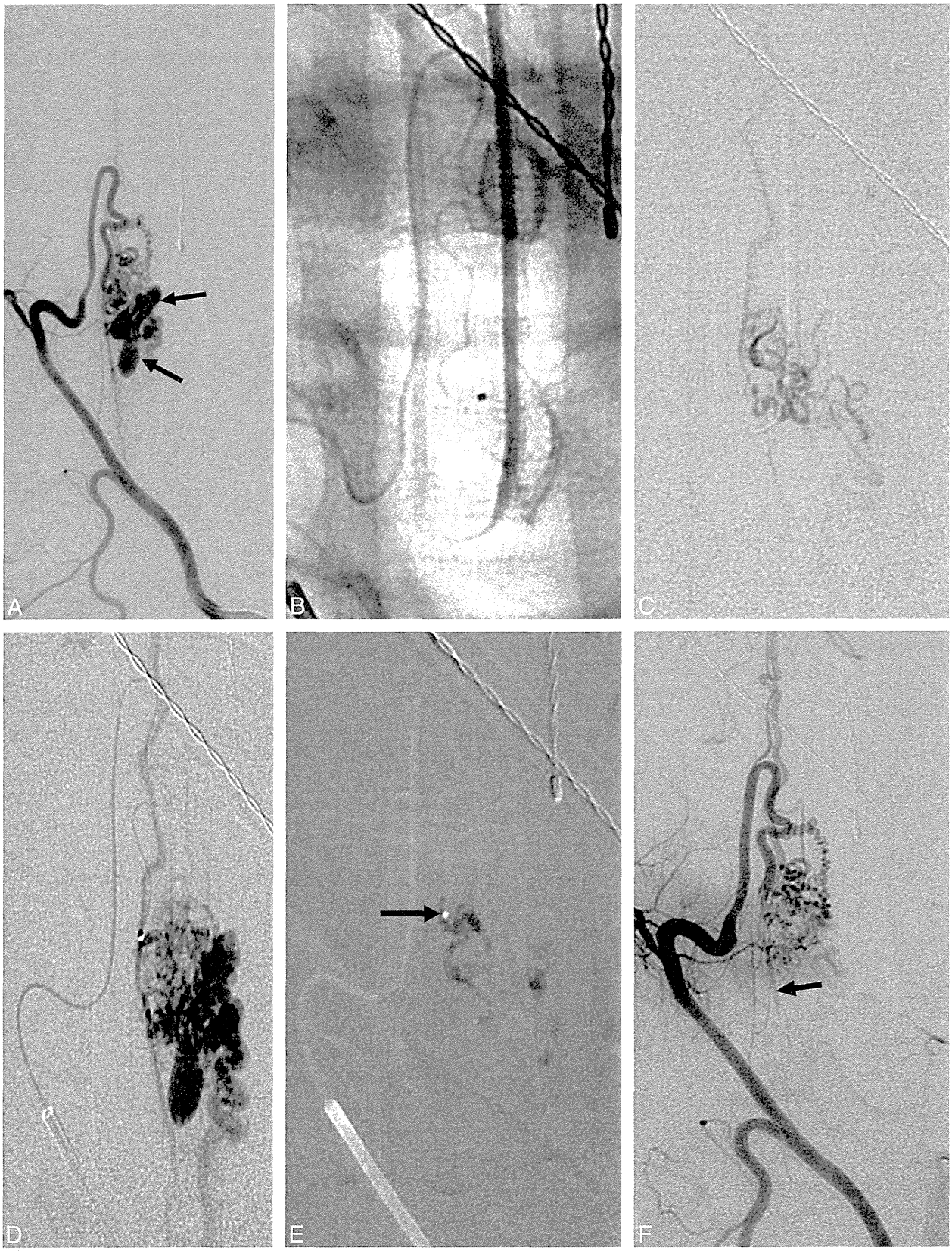

FIG 3. *A*, Posteroanterior view of the right T2 intercostal artery angiogram showing a nidus-type SCAVM supplied by the anterior spinal artery with multiple intranidal aneurysms (*arrows*). *B*, Nonsubtracted image of the microcatheter inserted into a feeder to the SCAVM. *C*, Superselective angiogram from the microcatheter inserted into the same feeder as *B*. No aneurysms are visualized. *D*, Superselective angiogram from a microcatheter placed in the ASA at the origin of the feeder to the SCAVM. Intranidal aneurysms and the distal anterior spinal artery are visualized. Embolization was performed from this catheter position using NBCA. *E*, Cast of NBCA. A small amount of NBCA is in the ASA axis near the catheter tip (*arrow*). *F*, Posteroanterior view of the right T2 intercostal artery after embolization. There is decreased visualization of the nidus without opacification of the intranidal aneurysms. The distal ASA is seen through the collateral (*arrow*).

monitoring with provocative testing provides additional safety, especially when vascular anatomy is modified by previous hemorrhage or treatment.[12] We prefer to use a flow-guided microcatheter for embolization because it is smaller in caliber and less traumatic to the blood vessel compared with a guidewire-assisted microcatheter. We prefer to use NBCA as an embolic agent because of its penetration small vessels and long-lasting occlusion effect. We try to reach the target as close as possible, but if not possible, we modify our technique to accomplish occlusion of the target as demonstrated in the illustrative case. We avoid embolization from a microcatheter wedged in a feeding artery because of the high risk of penetration of the embolic material into the normal territory or draining veins. The details of embolization techniques have been described elsewhere.[12,14] We proved that targeted embolization is beneficial to prevent recurrent hemorrhage even if it is partial treatment. We believe that endovascular embolization is the treatment of choice for most SCAVMs. The only exception is slow-flow, perimedullary AVFs located at the conus or filum terminale. It is important to obtain periodic clinical and radiologic follow-up and early endovascular intervention before significant deterioration occurs to obtain the best possible prognosis for SCAVMs.

Limitations

First, our study had a retrospective design with inherent limitations leading to potential ascertainment bias. Second, the number of patients was small, spread across many years, during which technical advancements were observed, though this may be unavoidable given that SCAVM is a rare disease. Third is the possibility of random error; overall, 13 univariate comparisons have been performed. Given the α level of .10, the high number of statistical tests makes it likely that 2 of the associations found may actually be the result of chance. Therefore, the interpretation of the results of univariate analysis was performed carefully, and the conclusion was performed by the multivariate analysis. As noted above, the results of the present study should be further clarified using an independent cohort would be difficult to perform given the rarity of SCAVMs.

CONCLUSIONS

The low rate of recurrent hemorrhage after endovascular treatment, compared with the high incidence of recurrent hemorrhage in conservative management, proves that endovascular treatment is effective to prevent hemorrhage.

REFERENCES

1. Veznedaroglu E, Nelson PK, Jabbour PM, et al. **Endovascular treatment of spinal cord arteriovenous malformations.** *Neurosurgery* 2006;59(5 suppl 3):S202–09; discussion S3–13 Medline
2. Kim LJ, Spetzler RF. **Classification and surgical management of spinal arteriovenous lesions: arteriovenous fistulae and arteriovenous malformations.** *Neurosurgery* 2006;59:S195–201; discussion S3–13 CrossRef Medline
3. Zozulya YP, Slin'ko EI, Al-Qashqish II. **Spinal arteriovenous malformations: new classification and surgical treatment.** *Neurosurg Focus* 2006;20:E7 Medline
4. Inagawa S, Yamashita S, Hiramatsu H, et al. **Clinical results after the multidisciplinary treatment of spinal arteriovenous fistulas.** *Jpn J Radiol* 2013;31:455–64 CrossRef Medline
5. Biondi A, Merland JJ, Reizine D, et al. **Embolization with particles in thoracic intramedullary arteriovenous malformations: long-term angiographic and clinical results.** *Radiology* 1990;177:651–58 CrossRef Medline
6. Rodesch G, Hurth M, Alvarez H, et al. **Angio-architecture of spinal cord arteriovenous shunts at presentation: clinical correlations in adults and children.** *Acta Neurochir (Wien)* 2004;146:217–26; discussion 226–27 CrossRef Medline
7. Biondi A, Merland JJ, Hodes JE, et al. **Aneurysms of spinal arteries associated with intramedullary arteriovenous malformations, II: results of AVM endovascular treatment and hemodynamic considerations.** *AJNR Am J Neuroradiol* 1992;13:923–31 Medline
8. Gross BA, Du R. **Spinal glomus (type II) arteriovenous malformations: a pooled analysis of hemorrhage risk and results of intervention.** *Neurosurgery* 2013;72:25–32; discussion 32 CrossRef Medline
9. Mourier KL, Gobin YP, George B, et al. **Intradural perimedullary arteriovenous fistulae: results of surgical and endovascular treatment in a series of 35 cases.** *Neurosurgery* 1993;32:885–91; discussion 891 Medline
10. Rosenblum B, Oldfield EH, Doppman JL, et al. **Spinal arteriovenous malformations: a comparison of dural arteriovenous fistulas and intradural AVM's in 81 patients.** *J Neurosurg* 1987;67:795–802 CrossRef Medline
11. von Elm E, Altman DG, Egger M, et al; STROBE Initiative. **The Strengthening the Reporting of Observational Studies in Epidemiology (STROBE) statement: guidelines for reporting observational studies.** *Lancet* 2007;370:1453–57 CrossRef Medline
12. Niimi Y, Sala F, Deletis V, et al. **Neurophysiologic monitoring and pharmacologic provocative testing for embolization of spinal cord arteriovenous malformations.** *AJNR Am J Neuroradiol* 2004;25:1131–38 Medline
13. Lasjaunias P. **A revised concept of the congenital nature of cerebral arteriovenous malformations.** *Interv Neuroradiol* 1997;3:275–81 CrossRef Medline
14. Berenstein A, Lasjaunias P, TerBrugge K. **Spinal arterioenous malformations.** In: *Surgical Neuroangiography.* Berlin Heidelberg: Springer-Verlag; 2004:737–847
15. Gross BA, Du R. **Spinal pial (type IV) arteriovenous fistulae: a systematic pooled analysis of demographics, hemorrhage risk, and treatment results.** *Neurosurgery* 2013;73:141–51; discussion 151 CrossRef Medline
16. Rodesch G, Hurth M, Alvarez H, et al. **Spinal cord intradural arteriovenous fistulae: anatomic, clinical, and therapeutic considerations in a series of 32 consecutive patients seen between 1981 and 2000 with emphasis on endovascular therapy.** *Neurosurgery* 2005;57:973–83; discussion 973–83 CrossRef Medline
17. Rodesch G, Hurth M, Alvarez H, et al. **Embolization of spinal cord arteriovenous shunts: morphological and clinical follow-up and results—review of 69 consecutive cases.** *Neurosurgery* 2003;53:40–49; discussion 49–50 CrossRef Medline
18. Konan AV, Raymond J, Roy D. **Transarterial embolization of aneurysms associated with spinal cord arteriovenous malformations: report of four cases.** *J Neurosurg* 1999;90(1 suppl):148–54 CrossRef Medline

J Orthop Sci (2015) 20:750–760
DOI 10.1007/s00776-015-0730-8

ORIGINAL ARTICLE

The societal burden of chronic pain in Japan: an internet survey

Tomoyuki Takura[1] · Takahiro Ushida[2] · Tsukasa Kanchiku[3] · Nozomi Ebata[4] · Koichi Fujii[4] · Marco daCosta DiBonaventura[5] · Toshihiko Taguchi[3]

Received: 17 September 2014 / Accepted: 19 February 2015 / Published online: 12 May 2015

Abstract

Objectives Chronic pain affects between 10–20 % of the population of Japan and several specific types of chronic pain have been found to be associated with worse health outcomes. The aim of the current study was to investigate the economic burden of chronic pain as well as the health status among Japanese patients.

Methods Data from the Japan National Health and Wellness Survey (NHWS), a cross-sectional health survey of adults, were used ($N = 30{,}000$). Respondents with chronic pain ($N = 785$) were compared with respondents without chronic pain ($N = 29{,}215$) with respect to health status (using the SF-12v2), work productivity and activity impairment (WPAI questionnaire), and healthcare resource use using regression modeling, controlling for demographic and health history covariates. Indirect costs were calculated using wage rates and the human capital method.

Results Back pain (72.10 %) and shoulder pain/stiffness (54.90 %) were the most prevalent pain types. Adjusting for demographic and health history differences, respondents with chronic pain reported lower health status [mental component summary (MCS): 44.26 vs. 51.14; physical component summary (PCS): 44.23 vs. 47.48; both $p < 0.05$], greater absenteeism (4.74 vs. 2.74 %), presenteeism (30.19 vs. 15.19 %), overall work impairment (31.70 vs. 16.82 %), indirect costs (¥1488,385 vs. ¥804,634), activity impairment (33.45 vs. 17.25 %), physician visits (9.31 vs. 4.08), emergency room (ER) visits (0.19 vs. 0.08), and hospitalizations (0.71 vs. 0.34) (all $p < 0.05$). Nearly 60 % of respondents with chronic pain were untreated. The mean level of pain severity in the last week was 5.26 (using a 0–11 scale); being female, being elderly, having low income, and having multiple pain types were significantly associated with greater pain severity (all $p < 0.05$). Regular exercise was associated with lower pain severity ($p < 0.05$).

Conclusions The results suggest that chronic pain has a significant association in an individual's health status, work productivity, daily activity impairment, healthcare resource use, and economic burden in Japan. Along with low treatment rates, a multidisciplinary approach may lead to an improved quality of life and reduce the economic burden among patients with chronic pain in Japan.

✉ Marco daCosta DiBonaventura
marco.dibonaventura@kantarhealth.com

[1] Department of Health Economics and Industrial Policy, Osaka University Graduate School of Medicine, Osaka, Japan

[2] Multidisciplinary Pain Center, Aichi Medical University, Nagakute, Japan

[3] Department of Orthopaedic Surgery, Yamaguchi University Graduate School of Medicine, Yamaguchi, Japan

[4] Pain/Neuroscience Medical Affairs, Pfizer, Tokyo, Japan

[5] Health Outcomes Practice, Kantar Health, 11 Madison Avenue, 12th Floor, New York, NY 10010, USA

Introduction

The prevalence of chronic pain, defined as pain lasting at least three months [1], varies between 11.5 and 55.2 % among Western nations [2]. The rates in Japan have been found to be similar. A recent (2011) study of 20,000 adults aged 20–69 years reported that 26.4 % met the criteria for chronic pain [3]. According to the Institute of Medicine, rates of chronic pain are expected to increase due to increases in other chronic conditions which co-occur with pain (e.g., cancer), increases in obesity, improved

management of catastrophic injuries (which will reduce mortality but increase the number of survivors with chronic pain), and greater awareness on the part of the patient about chronic pain and treatment options [4].

Evidence from the Western literature suggests significant effects of chronic pain on quality of life, activities of daily living, productivity, suicide risk, and indirect and direct costs [4–6]. Using a nationwide mailed survey in Japan, Nakamura et al. [7] found that respondents who reported experiencing musculoskeletal pain also reported more work-related effects, more impairment in daily activities, and lower health status as assessed by the Short Form-36 (SF-36). Another study using a home visit survey of the elderly in Takasaki City, found that the presence of chronic knee pain was associated with significantly increased impairments in activities of daily living [8]. Recently, DiBonaventura et al. [9] compared respondents with neuropathic pain with controls, adjusting for comorbidities and other variables using the Japan National Health and Wellness Survey, and found that chronic neuropathic pain was associated with lower health status and greater work-related impairment and healthcare resource use. Aside from physical limitations, other studies have documented the relationship between pain and psychological illness [10].

However, much of the chronic pain research in Japan has been limited by a focus on specific types of pain (e.g., neuropathic, musculoskeletal, knee, etc.), and the evidence of the economic burden of chronic pain among Japanese patients is quite limited. Therefore, the aim of the current work was to more broadly examine the types of chronic pain experienced and its collective burden in Japan by assessing both humanistic and economic effects. Specifically, the present study explored the association between chronic pain and health status, work productivity loss, healthcare resource utilization, and indirect costs in a nationwide sample. A secondary aim was to understand what factors were most strongly associated with greater pain severity among those with chronic pain.

Methods

Data source and procedures

Data from the 2011 Japan National Health and Wellness Survey (NHWS) were used in the analyses. The NHWS is an Internet survey administered to adults in Japan from November to December, 2011. The NHWS is a purely patient-reported survey which includes information on sociodemographics, general health history, medical comorbidities, medication usage, and health outcomes, among other variables. NHWS respondents are members of the Lightspeed Research (LSR) panel or its partners, which are opt-in survey panels with a total of over 4 million members worldwide. Members of LSR and its partners were recruited through an opt-in email, co-registration with LSR partners, an e-newsletter campaigns, and online banner placements. All potential panel members must register with a unique email address and password and complete an in-depth demographic registration profile.

Panel members were not recruited from a purely convenience-of-sampling standpoint; some attempts were made to equate the panel membership with basic census information. For example, in Japan 52 % of the population is female and 32 % of the population reports an annual income of <¥4 million; 49 % and 31 % of the panel are female and have an annual income of <¥4 million, respectively [11]. Nevertheless, the characteristics of the panel do not entirely match that of the population and skew toward being a younger population.

The NHWS recruits from this panel in stratified random sample (by sex and age) was implemented to mitigate some of these biases by ensuring the final NHWS sample is demographically consistent with the Japanese adult population based on governmental statistics [12]. Specifically, by using the international database of the U.S. Census, the distribution of age and sex in Japan was identified and mimicked such that the final NHWS sample ($N = 30{,}000$; response rate = 15.33 %) matches these distributions. Although not included in the sampling frame, distributions of household income and region are also consistent between the NHWS data and the governmental statistics of Japan [12]. All respondents provided informed consent and the study protocol was reviewed and approved by an institutional review board. Respondents received modest compensation in exchange for their participation.

Sample

The total sample in the 2011 Japan NHWS is 30,000 respondents. All respondents were included in the analyses.

Measures

Chronic pain

All respondents in the NHWS were asked whether they experienced pain in the past 12 months. For those who answered affirmatively, they were then asked if they experienced pain in the past month. For those who answered affirmatively, they were presented with a list of types of pain and asked which they had experienced and whether those types of pain were diagnosed. If they were diagnosed, respondents were asked how long they experienced each type of pain. From all this information, a dichotomous group variable (having chronic pain vs. not having chronic

pain) was used as the primary predictor of study outcomes. Chronic pain was defined as experiencing one of the following types of pain for three months or more: arthritis, back problems, cancer, fibromyalgia, joint, neck, neuropathic (including diabetic peripheral neuropathy), postherpetic neuralgia, shoulder, sprain/strain, surgery/medical procedure, or phantom limb pain. Those that did not meet the definition for chronic pain were considered to not have chronic pain. Patients with chronic pain were asked to evaluate their level of severity for each type of pain ("mild", "moderate", or "severe") and also asked to provide an overall assessment of their pain severity in the last week using an 11-point numeric rating scale (NRS-11; with 0 representing no pain, to 10 representing the worst pain imaginable). Patients were also asked whether they were currently taking a prescription medication at the time of the survey (yes vs. no).

Sociodemographics

The sex, age, marital status (married/living with partner vs. not-married), education (university educated vs. less than university educated), annual household income (<¥3,000,000, ¥3,000,000 to <¥5,000,000, ¥5,000,000 to <¥8,000,000, ≥¥8,000,000, or decline to answer), and employment status (currently employed or not currently employed) were assessed and considered as covariates. Household composition (living alone, living with adults only, living with children and adults, or living with children only) was also included as an additional variable in lieu of marital status in certain analyses.

Health history

Smoking status (currently smoke vs. do not currently smoke), alcohol use (currently drink vs. do not currently drink), and exercise behavior (currently exercise vs. do not currently exercise) were assessed and used as covariates in regression analyses. Height and weight were converted to body mass index (BMI) with the following categories: <18.5 kg/m^2 (i.e., underweight), 18.5 to <25.0 kg/m^2 (i.e., normal BMI), ≥25.0 kg/m^2 (i.e., obese), or decline to provide weight. The Charlson comorbidity index (CCI) was also included and calculated by weighting the presence of a variety of chronic conditions and summing the result with greater total index scores indicating a greater comorbid burden on the respondent [13].

Health status

The Medical Outcomes Study 12-Item Short Form Survey Instrument (SF-12v2) is a multipurpose, generic health status instrument [14]. The items from the SF-12v2 are used to calculate two normed summary scores: physical component summary (PCS) and mental component summary (MCS). The SF-12v2 items can also be used to generate health state utilities, which represents the preference for a particular health state and varies conceptually from 0 (a state equivalent to death) to 1 (a state equivalent to perfect health). This conversion is achieved through application of the SF-6D classification [15]. For all SF-12v2-derived measures, higher scores indicate better health status.

Work productivity and activity impairment

Work productivity was assessed using the general health version of the Work Productivity and Activity Impairment (WPAI-GH) questionnaire, a 6-item validated instrument, which consists of four metrics: absenteeism (the percentage of work time missed because of one's health in the past seven days), presenteeism (the percentage of impairment experienced while at work in the past seven days because of one's health), overall work productivity loss (an overall impairment estimate that is a combination of absenteeism and presenteeism), and activity impairment (the percentage of impairment in daily activities because of one's health in the past seven days) [16]. Absenteeism, presenteeism, and overall work productivity loss were only calculated for respondents who were employed.

Healthcare resource use

Healthcare utilization was defined by the number of traditional healthcare provider visits, the number of emergency room (ER) visits ("How many times have you been to the ER for your own medical condition in the past six months?"), and the number of times hospitalized ("How many times have you been hospitalized for your own medical condition in the past six months?") for all medical conditions experienced in the past six months.

Statistical analyses

Differences between those with and without chronic pain were examined with respect to demographics and health characteristics using Chi square tests (categorical outcomes) and analysis of variance (ANOVA) tests (continuous outcomes). Differences between those with and without chronic pain were then examined with respect to health outcomes (i.e., health status, work productivity and activity impairment, and healthcare resource use) using regression modeling, controlling for age, gender, household income, BMI, smoking status, exercise behavior, and the CCI. These covariates were chosen because they differed between those with chronic pain and those without chronic pain and have known associations with health outcomes in Japan [12].

General linear models were used for health status variables due to the normality of the distribution. Aside from reporting the unstandardized regression estimate (b) for the effect of pain (which indicate the difference in the dependent variable between those with and without chronic pain, holding all covariates constant), adjusted means were also reported from these models using a least squares algorithm, setting each covariate to the mean of the analytical sample. Generalized linear models were used for work productivity and healthcare resource use variables due to their pronounced skew. A negative binomial distribution provided the best fit for the work productivity, activity impairment, and healthcare resource use variables due to the skewed distributions and a multiplicative dispersion parameter being added to adjust the standard errors because of a slight model underdispersion. Unstandardized regression estimates (b) as well as the anti-log of b (i.e., e^b or rate ratios) were presented for the effect of pain. Rate ratios represent the multiplicative factor for which the mean of the pain group is greater than that of the control group (e.g., a rate ratio of 1.30 indicates the mean for the pain group is 1.30 times that of the control group). In addition, adjusted means were also reported from these models using a maximum likelihood algorithm, setting each covariate to the mean of the analytical sample.

Annual costs due to absenteeism and presenteeism were calculated by integrating information from the WPAI and hourly wage rates from the Japan Basic Survey on Wage Structure [17] using the human capital method. For each employed respondent, his or her hours lost due to either absenteeism or presenteeism (measured using the WPAI instrument) were then multiplied by their estimated wage (based on age and sex) to estimate total weekly indirect costs. These figures were then annualized. The presence of chronic pain was then used to predict these total indirect costs using a generalized linear model (again, with a negative binomial distribution and a log-link function to best capture the skewness of the data) controlling for age, sex, household income, BMI, smoking status, exercise behavior, and the CCI. Adjusted means were reported from these models using a maximum likelihood algorithm, setting each covariate to the mean of the analytical sample.

To further illustrate the burden of chronic pain, an additional analysis was performed comparing those with chronic pain to those with non-chronic pain (i.e., those without any pain from the control group in the main analysis were excluded from the control group in this supplemental analysis). This approach would isolate the effect of chronic pain on health outcomes above and beyond any effect of general non-chronic pain. Aside from excluding respondents without pain from the control group, this supplemental analysis replicated the exact approach in the main analysis described above. The same outcomes were examined and the same modeling procedure was used.

To examine the secondary objective, overall pain severity in the last week was predicted using the available sociodemographic and health history variables in a general linear model. In this model, the same covariates were coded and used as described above with the following exceptions: age was categorized in ten-year increments as opposed to entered continuously (to best understand the age groups with the highest pain severity), household composition was used in lieu of marital status, and the number of pain types (1, 2, 3, or 4+) was used as an additional predictor.

All analyses were conducted using SAS version 9.3 (Cary, NC).

Results

A total of 785 respondents met our criteria for chronic pain (2.62 %). Demographic and health characteristics for respondents with and without chronic pain are shown in Table 1. Respondents with chronic pain were significantly more likely to be older, be female, be unemployed, exercise regularly, and have a greater BMI and comorbidity burden compared with those without chronic pain (all $p < 0.05$).

Among respondents who reported chronic pain, the types of pain experienced in the past month and types of pain diagnosed are shown in Table 2. Both back pain (72.10 %) and shoulder pain/stiffness (54.90 %) were the most prevalent pain types and were experienced by more than half of respondents with chronic pain. A total of 41.02 % respondents reported they were currently using a prescription medication for their pain. However, there was considerable variability in treatment rates across pain types, as shown in Table 2. Despite the small sample size (which creates additional uncertainty around these estimates), broken bones (71.43 %), cancer pain (66.67 %), and phantom limb pain (66.67 %) were the most likely pain types to be treated. Conversely, menstrual cycle pain (38.60 %), back pain (40.81 %), and post-herpetic neuralgia (40.91 %) were the pain types least likely to be treated.

Analyses were then conducted to compare the health outcomes of those with and without chronic pain using regression analysis. Respondents with chronic pain reported significantly lower levels of MCS [b (unstandardized regression estimate) $= -3.24$, $p < 0.05$] and PCS ($b = -6.88$, $p < 0.05$) relative to respondents without chronic pain (both $p < 0.05$). Figure 1 shows the adjusted means for MCS (44.26 vs. 51.14 for chronic pain and controls, respectively) and PCS scores (44.23 vs. 47.48 for chronic pain and controls, respectively). Additionally, those with chronic pain reported significantly lower levels of health utilities ($b = -0.09$, $p < 0.05$; Adjusted means = 0.68 vs. 0.77 for those with and without chronic pain, respectively).

Table 1 Demographic and health characteristics in those with and without chronic pain

	Total ($N = 30,000$)	Chronic pain ($N = 785$)	No chronic pain ($N = 29,215$)	p
Age (years)				
Mean ± SD	47.38 ± 15.63	53.97 ± 13.78	47.20 ± 15.64	<0.001
Gender				
Female (%)	14,958 (49.9 %)	428 (54.5 %)	14,530 (49.7 %)	0.008
Male (%)	15,042 (50.1 %)	357 (45.5 %)	14,685 (50.3 %)	
Education level				
Less than university education (%)	15,912 (53.0 %)	422 (53.8 %)	15,490 (53.0 %)	0.683
University education or higher (%)	14,088 (47.0 %)	363 (46.2 %)	13,725 (47.0 %)	
Household composition				
Live alone (%)	4466 (14.9 %)	111 (14.1 %)	4355 (14.9 %)	0.047
Live with children only (%)	375 (1.3 %)	15 (1.9 %)	360 (1.2 %)	
Live with adults only (%)	17,538 (58.5 %)	485 (61.8 %)	17,053 (58.4 %)	
Live with adults and children (%)	7621 (25.4 %)	174 (22.2 %)	7477 (25.5 %)	
Annual household income				
<¥3 million (%)	5143 (17.1 %)	152 (19.4 %)	4991 (17.1 %)	<0.001
¥3 million to <¥5 million (%)	7571 (25.2 %)	204 (26.0 %)	7367 (25.2 %)	
¥5 million to <¥8 million (%)	7664 (25.5 %)	179 (22.8 %)	7485 (25.6 %)	
¥8 million or more (%)	6586 (22.0 %)	201 (25.6 %)	6385 (21.9 %)	
Decline to answer (%)	3036 (10.1 %)	49 (6.2 %)	2987 (10.2 %)	
Employment status				
Not currently employed (%)	12,180 (40.6 %)	365 (46.5 %)	11,815 (40.4 %)	<0.001
Employed (%)	17,820 (59.4 %)	420 (53.5 %)	17,400 (59.6 %)	
Body mass index (BMI) category				
Underweight (%)	3131 (10.4 %)	65 (8.3 %)	3066 (10.5 %)	<0.001
Acceptable risk (%)	15,197 (50.7 %)	350 (44.6 %)	14,847 (50.8 %)	
Increased risk (%)	8309 (27.7 %)	259 (33.0 %)	8050 (27.6 %)	
High risk (%)	2147 (7.2 %)	98 (12.5 %)	2049 (7.0 %)	
Decline to provide weight (%)	1216 (4.1 %)	13 (1.7 %)	1203 (4.1 %)	
Alcohol use				
Do not drink (%)	8485 (28.3 %)	217 (27.6 %)	8268 (28.3 %)	0.687
Drink alcohol (%)	21515 (71.7 %)	568 (72.4 %)	20947 (71.7 %)	
Smoking behavior				
Never smoked (%)	16780 (55.9 %)	375 (47.8 %)	16405 (56.2 %)	<0.001
Former smoker (%)	7057 (23.5 %)	241 (30.7 %)	6816 (23.3 %)	
Current smoker (%)	6163 (20.5 %)	169 (21.5 %)	5994 (20.5 %)	
Exercise behavior				
Do not exercise (%)	16443 (54.8 %)	372 (47.4 %)	16071 (55.0 %)	<0.001
Regularly exercise (%)	13557 (45.2 %)	413 (52.6 %)	13144 (45.0 %)	
Charlson comorbidity index				
Mean ± SD	0.15 ± 0.58	0.49 ± 1.82	0.14 ± 0.50	<0.001

Those with chronic pain also reported significantly higher levels of absenteeism ($b = 0.55$, rate ratio = 1.73, $p < 0.05$), presenteeism ($b = 0.69$, rate ratio = 1.99, $p < 0.05$), overall work impairment ($b = 0.63$, rate ratio = 1.89, $p < 0.05$), and activity impairment ($b = 0.66$, rate ratio = 1.94, $p < 0.05$). Figure 2 shows the associated adjusted means for these outcomes (absenteeism: 4.74 vs. 2.74 %; presenteeism: 30.19 vs. 15.19 %; overall work impairment: 31.70 vs. 16.82 %; and activity impairment: 33.45 vs. 17.25 %) for those with and without chronic pain, respectively (all $p < 0.05$).

Differences in absenteeism and presenteeism were then converted to annual costs in Fig. 3. Adjusting for confounding variables, employed patients with chronic

Table 2 Types of pain experienced, diagnosed, and treated, and levels of pain severity among those with chronic pain ($N = 785$)

Pain type	Experienced in the past month (among all patients, $N = 785$)		Using a prescription medication (among patients with that particular type of pain)		Diagnosed (among all patients, $N = 785$)		Severity of pain experienced in the past month					
							Mild		Moderate		Severe	
	n	%	*n*	%	*n*	%	*n*	%	*n*	%	*n*	%
Back problems	566	72.10	231	40.81	477	60.76	241	42.58	253	44.70	72	12.72
Shoulder pain/stiffness	431	54.90	179	41.53	233	29.68	185	42.92	185	42.92	61	14.15
Joint pain	252	32.10	108	42.86	180	22.93	128	50.79	100	39.68	24	9.52
Neck	208	26.50	98	47.12	112	14.27	90	43.27	90	43.27	28	13.46
Arthritis	191	24.33	80	41.88	154	19.62	111	58.12	63	32.98	17	8.90
Headache	164	20.89	77	46.95	53	6.75	91	55.49	64	39.02	9	5.49
Migraine	115	14.65	56	48.70	46	5.86	51	44.35	53	46.09	11	9.57
Dental problems	57	13.32	22	38.60	16	3.74	45	73.77	13	21.31	3	4.92
Menstrual cycle	61	7.77	25	40.98	45	5.73	29	50.88	17	29.82	11	19.30
Sprains/strains	50	6.37	23	46.00	31	3.95	39	78.00	8	16.00	3	6.00
Neuropathic pain (including DPN)	26	3.31	13	50.00	29	3.69	12	37.50	16	50.00	4	12.50
Post-herpetic neuralgia	22	2.80	9	40.91	18	2.29	14	63.64	5	22.73	3	13.64
Surgery/medical procedure	22	2.80	15	68.18	21	2.68	9	40.91	6	27.27	7	31.82
Fibromyalgia	18	2.29	8	44.44	22	2.80	9	45.00	8	40.00	3	15.00
Broken bones	14	1.78	10	71.43	12	1.53	7	50.00	7	50.00	0	0.00
Cancer	6	0.76	4	66.67	6	0.76	4	66.67	2	33.33	0	0.00
Phantom limb pain	6	0.76	4	66.67	3	0.38	2	33.33	3	50.00	1	16.67

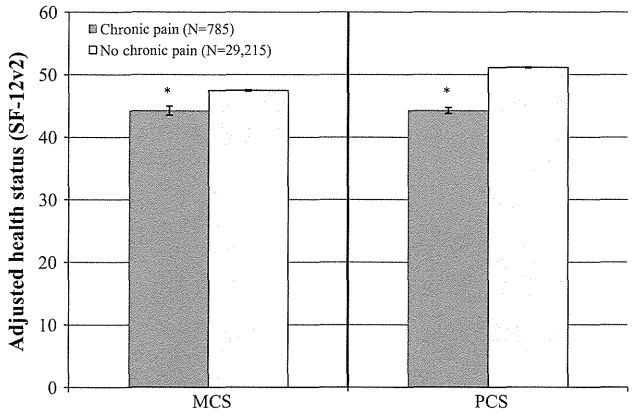

Fig. 1 Adjusted means of physical and mental health component summary scores among those with and without chronic pain. *$p < 0.05$ relative to the no chronic pain group (based on a t test of the chronic pain parameter estimate in the general linear model); *error bars* represents 95 % confidence intervals. *PCS* physical component summary and *MCS* mental component summary of the SF-12v2. All models controlled for age, sex, household income, body mass index, smoking status, alcohol use, exercise behavior, and the Charlson comorbidity index

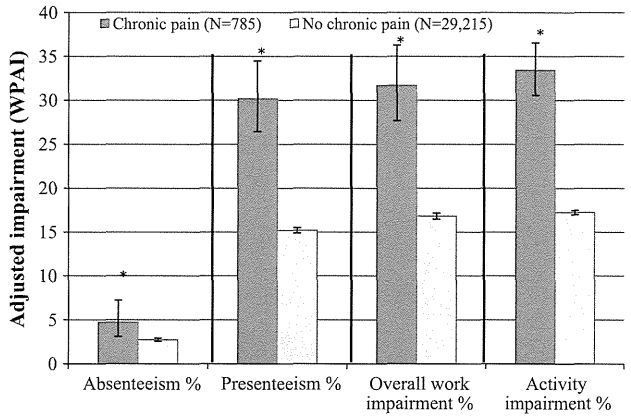

Fig. 2 Adjusted means of work productivity and activity impairment among those with and without chronic pain. *$p < 0.05$ relative to the no chronic pain group (based on a z test of the chronic pain parameter estimate in the generalized linear model); *error bars* represents 95 % confidence intervals. Only those employed full or part-time ($n = 17{,}820$) provided data for absenteeism, presenteeism, and overall work impairment. All models controlled for age, sex, household income, body mass index, smoking status, alcohol use, exercise behavior, and the Charlson comorbidity index

pain had ¥232,815 in lost wages due to absenteeism per-patient per-year compared with ¥139,330 for employed respondents without chronic pain ($p < 0.05$). Similarly, employed patients with chronic pain had ¥1,255,570 in lost wages due to presenteeism per-patient per-year compared with ¥665,304 for employed respondents without chronic pain ($p < 0.05$). The total indirect costs for employed patients with chronic pain were significantly higher than

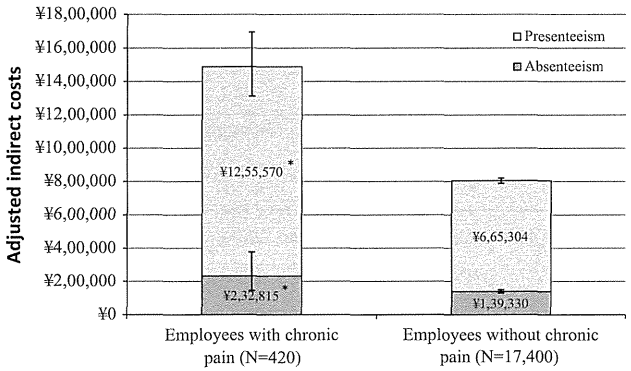

Fig. 3 Adjusted means of indirect costs among those with and without chronic pain. *$p < 0.05$ relative to the no chronic pain group (based on a z test of the chronic pain parameter estimate in the generalized linear model); *error bars* represents 95 % confidence intervals. All models controlled for age, sex, household income, body mass index, smoking status, alcohol use, exercise behavior, and the Charlson comorbidity index

employed respondents without chronic pain (¥1,488,385 vs. ¥804,634, $p < 0.05$).

Similar relationships were observed when predicting healthcare resource use. Chronic pain was associated with an increased number of physician visits ($b = 0.83$, rate ratio $= 2.29$, $p < 0.05$), ER visits ($b = 0.86$, rate ratio $= 2.37$, $p < 0.05$), and hospitalizations ($b = 0.74$, rate ratio $= 2.10$, $p < 0.05$). The adjusted means of these models are shown in Fig. 4. In all cases, the adjusted means were more than twice as high for respondents with chronic pain: physician visits = 9.31 vs. 4.08, ER visits = 0.19 vs. 0.08, and hospitalizations = 0.71 vs. 0.34 (all $p < 0.05$).

Severity of pain experienced in the past month for each specific pain type was examined among those with chronic pain, as shown in Table 2. For most types of pain, between 40–60 % of respondents reported their pain as moderate-to-severe. The highest proportion of severe pain was experienced in relation to surgery/medical procedure pain (31.82 %). A majority of respondents experiencing chronic pain reported not being treated for their pain ($n = 463$, 58.98 %).

As discussed in the statistical analysis section above, a supplemental analysis was performed to compare health outcomes between respondents with chronic pain ($N = 785$) and respondents with non-chronic pain ($N = 3219$). Adjusting for the same set of covariates as noted in the main analysis, a similar pattern of results was observed (see Table 3). Although adjusted MCS scores were not significantly different between groups (44.04 vs. 44.41 for chronic pain and non-chronic pain, respectively; $p = 0.38$), PCS scores and health utilities were significantly lower among those with chronic pain (both $p < 0.05$). Similarly, all forms of work impairment, activity impairment, and healthcare resource use were significantly higher among those with chronic pain compared with those with non-chronic pain (all $p < 0.05$). Levels of impairment and healthcare resource use were generally 50 % higher among those with chronic pain.

Further, employed patients with chronic pain had ¥218,424 in lost wages due to absenteeism per-patient per-year compared with ¥121,339 for employed respondents with non-chronic pain ($p < 0.05$). Similarly, employed patients with chronic pain had ¥1,300,077 in lost wages

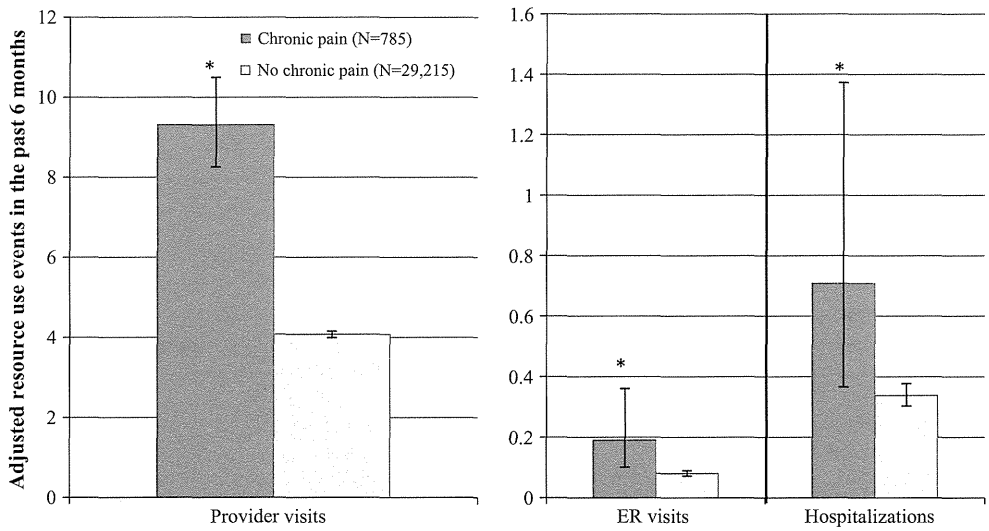

Fig. 4 Adjusted means of healthcare resource use among those with and without chronic pain. *$p < 0.05$ relative to the no chronic pain group (based on a z test of the chronic pain parameter estimate in the generalized linear model); *error bars* represents 95 % confidence intervals. All models controlled for age, sex, household income, body mass index, smoking status, alcohol use, exercise behavior, and the Charlson comorbidity index